

Diagonalization- and Numerical Renormalization-Group-based Methods for Interacting Quantum Systems

Reinhard M. Noack

Fachbereich Physik

Philipps-Universität Marburg, Germany

IX Training Course in the Physics of Correlated Electron Systems and High- T_c Superconductors

Vietri sul Mare, 11-15 October 2004

Literature:

- *Density Matrix Renormalization: A New Numerical Method in Physics*, Eds. I. Peschel, X. Wang, M. Kaulke, and K. Hallberg, Springer Verlag, Berlin, June 1999.
- E. Dagotto, “Correlated electrons in high-temperature superconductors”, *Rev. Mod. Phys.* **66**, 763-840 (1994).
- A. Booten and H. van der Vorst, “Cracking large-scale eigenvalue problems, part I: Algorithms”, *Computers in Phys.* **10**, No. 3, p. 239 (May/June 1996); “Cracking large-scale eigenvalue problems, part II: Implementations”, *Computers in Phys.* **10**, No. 4, p. 331 (July/August 1996).
- N. Laflorencie and D. Poilblanc, “Simulations of pure and doped low-dimensional spin-1/2 gapped systems”, [cond-mat/0408363](#).
- K. G. Wilson, “The renormalization group and critical phenomena”, *Rev. Mod. Phys.* **55**, 583-600 (1983).
- U. Schollwöck, “The density-matrix renormalization group”, [cond-mat/0409292](#), to appear in *Rev. Mod. Phys.*
- W.H. Press, S.A. Teukolsky, W.T. Vetterling, and B.P. Flannery, *Numerical Recipes in C [or C++]*, 2nd ed., Cambridge University Press (1993).

Outline

I. Exact Diagonalization

- (i) Introduction to interacting quantum systems
- (ii) Representation of many-body states
- (iii) Complete Diagonalization
- (iv) Iterative Diagonalization (Lanczos and Davidson)
- (v) Dynamics
- (vi) Finite temperature

II. Numerical Renormalization Group

- (i) Anderson and Kondo problems
- (ii) Numerical RG for the Kondo problem
- (iii) Numerical RG for quantum lattice problems
- (iv) Numerical RG for a noninteracting particle

III. From the NRG to the Density Matrix Renormalization Group

- (i) Better methods for the noninteracting particle
- (ii) Density Matrix Projection for interacting systems
- (iii) DMRG Algorithms
- (iv) DMRG-like algorithm for the noninteracting particle

IV. The DMRG in Detail

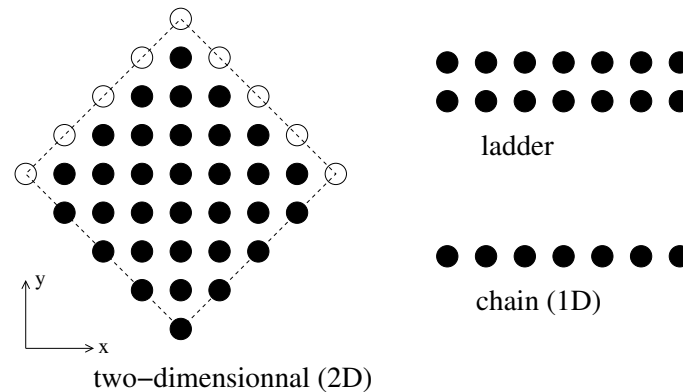
- (i) Programming details
- (ii) Measurements
- (iii) Wavefunction transformations
- (iv) Extensions to higher dimension

V. Recent Developments in the DMRG

- (i)* Classical transfer matrices
- (ii)* Finite temperature
- (iii)* Dynamics
- (iv)* Quantum chemistry
- (v)* Time evolution
- (vi)* Matrix product states
- (vii)* Quantum information

I. Exact Diagonalization

Direct diagonalization of Hamiltonian matrix on finite clusters



Goals

- ground state properties
- low-lying excitations
- dynamics, finite T , ...

Advantages

- almost any system can be treated
- almost any observable can be calculated
- quantum-number resolved quantities
- numerically exact (for finite cluster)

Limitation: exponential in lattice size

Largest sizes reached

- $S = 1/2$ spin models
square lattice: $N = 40$ triangular lattice: $N = 39$, star lattice: $N = 42$
maximum dimension of basis: 1.5 billion
- t - J models
checkerboard lattice with 2 holes: $N = 32$
square lattice with 2 holes: $N = 32$
maximum dimension of basis: 2.8 billion
- Hubbard models
square lattice at half filling: $N = 20$
quantum dot structure: $N = 20$
maximum dimension of basis: 3 billion
- Holstein models
chain with $N = 14$ + phonon pseudo-sites
maximum dimension of basis: 30 billion

I (i) Interacting Quantum Systems

Here: discrete, finite case

- system of N quantum mechanical subsystems, $\ell = 1, \dots, N$
- finite number of basis states per subsystem

$$|\alpha_\ell\rangle, \quad \alpha_\ell = 1, \dots, s_\ell$$

- more general case: $s_\ell \rightarrow \infty$ (continuum or thermodynamic limit)
 $N \rightarrow \infty$ (thermodynamic limit)
 $\ell \rightarrow x$ (continuous quantum field)

Properties:

- Basis *direct product* of component basis

$$|\alpha_1, \alpha_2, \dots, \alpha_N\rangle \equiv |\alpha_1\rangle \otimes |\alpha_2\rangle \otimes \dots \otimes |\alpha_N\rangle$$

\Rightarrow total number of states: $\prod_{\ell=1}^N s_\ell$

- arbitrary state in this basis

$$|\psi\rangle = \sum_{\{\alpha_\ell\}} \psi(\alpha_1, \alpha_2, \dots, \alpha_N) |\alpha_1, \alpha_2, \dots, \alpha_N\rangle$$

- behavior governed by Schrödinger equation

$$H |\Psi(t)\rangle = i\hbar \frac{\partial}{\partial t} |\Psi(t)\rangle \quad \text{or} \quad H |\psi\rangle = E |\psi\rangle \quad (\text{time-independent})$$

Hamiltonians

In general, Hamiltonians can connect arbitrary numbers of subsystems

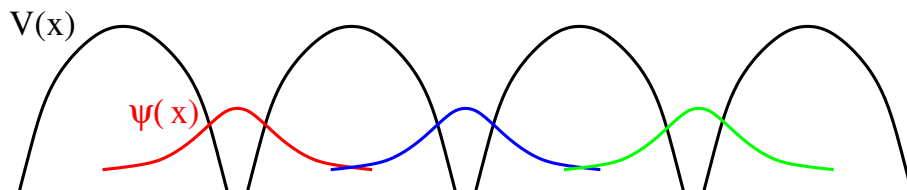
$$H = \sum_{\ell} H_{\ell}^{(1)} + \sum_{\ell, m} H_{\ell m}^{(2)} + \dots + \sum_{\ell, m, p} H_{\ell m n p}^{(4)} + \dots$$

- $H_{\ell}^{(1)}$ usually determines $|\alpha_{\ell}\rangle$
- $H_{\ell m}^{(2)}$, sometimes $H_{\ell m n p}^{(4)}$ will be important here
- $H_{\ell m}^{(2)}$ often short-ranged

Typical terms:

- tight-binding term:

$$H^{\text{tb}} = - \sum_{\ell, m, \sigma} t_{\ell m} c_{\ell, \sigma}^{\dagger} c_{m, \sigma}$$



- localized Wannier orbitals (unfilled d - or f - orbitals in transition metals)
- states $|0\rangle, |\uparrow\rangle, |\downarrow\rangle, |\uparrow\downarrow\rangle$ per orbital $\rightarrow 4^N$ degrees of freedom
- overlap between near orbitals – “hopping” $t_{\ell m}$ short ranged (n.n., possibly n.n.n.)

- local (Anderson) disorder

$$H_\ell^A = \sum_\sigma \lambda_\ell n_{\ell,\sigma} \quad , \quad n_{\ell,\sigma} \equiv c_{\ell,\sigma}^\dagger c_{\ell,\sigma}$$

- Coulomb interaction between electrons

$$H_{\ell m}^C = \frac{e^2}{|\mathbf{r}_\ell - \mathbf{r}_m|}$$

screening leads to

- on-site (Hubbard) interaction

$$H_\ell^U = U n_{\ell,\uparrow} n_{\ell,\downarrow}$$

- near-neighbor Coulomb interaction

$$H_{\ell m}^V = V n_\ell n_{\ell+\hat{\mathbf{r}}} \quad , \quad (n_\ell \equiv \sum_\sigma n_{\ell,\sigma}) \quad \text{etc.}$$

- Spin models

- \mathbf{S}_i localized quantum mechanical spins ($S = 1/2, 1, 3/2, \dots$)
states $| -S \rangle | -S + 1 \rangle \dots | S \rangle \Rightarrow (2S + 1)^N$ degrees of freedom

- Heisenberg exchange

$$H_{\ell m}^{\text{Heis}} = J \mathbf{S}_\ell \cdot \mathbf{S}_m = J^z S_\ell^z S_m^z + \frac{1}{2} J^{xy} (S_\ell^+ S_m^- + S_\ell^- S_m^+)$$

- strong coupling limit of the Hubbard model at $n = 1$ ($S = 1/2$)



- variations: $J^z \neq J^{xy}$ (Ising or XY anisotropy), $H_\ell^n = D(S_\ell^z)^2$ (single-ion),

$$H_{\ell m}^{bq} = J_2 (\mathbf{S}_\ell \cdot \mathbf{S}_m)^2 \quad (\text{biquadratic})$$

- t - J model: strong-coupling limit of doped Hubbard

$$H_{\ell m}^{tJ} = \mathcal{P} H_{\ell m}^{tb} \mathcal{P} + J \left(\mathbf{S}_\ell \cdot \mathbf{S}_m - \frac{1}{4} n_\ell n_m \right)$$

double occupancy projected out (\mathcal{P}) - 3 states/site

- Anderson impurity - hybridized d (or f) orbital with on-site interaction

$$H_\ell^{AI} = \varepsilon_d n_\ell^d + V \left(d_{\ell,\sigma}^\dagger c_{\ell,\sigma} + \text{H.c.} \right) + U n_{\ell,\downarrow}^d n_{\ell,\downarrow}^d$$

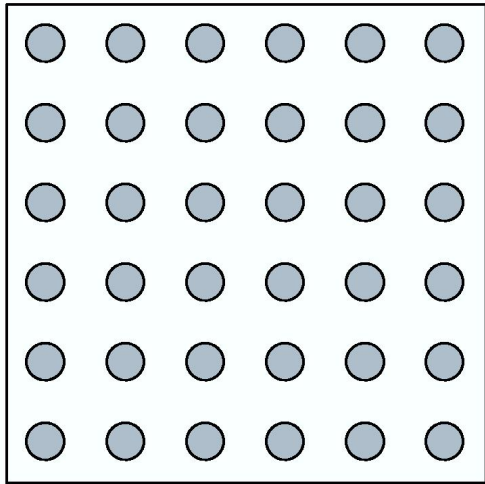
single impurity or lattice (PAM) possible

- Kondo impurity - localized d spin \mathbf{S}

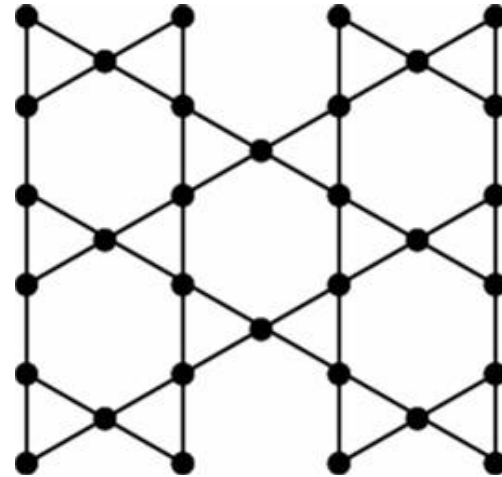
$$H_\ell^K = \frac{J_K}{2} \mathbf{S}_\ell \cdot \left(c_{\ell,\alpha}^\dagger \boldsymbol{\sigma}_{\alpha,\beta} c_{\ell,\beta} \right)$$

limit of symmetric Anderson impurity at strong U

Lattices



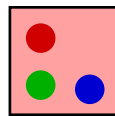
square lattice



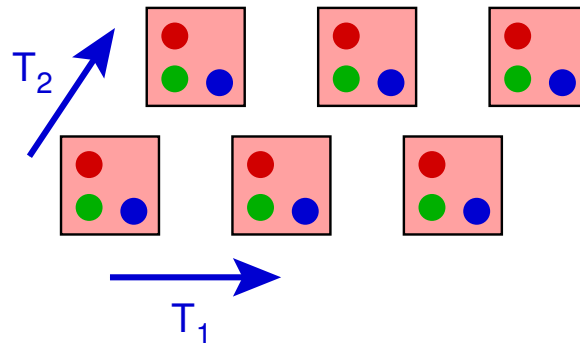
Kagomé lattice

Described by

- unit cell

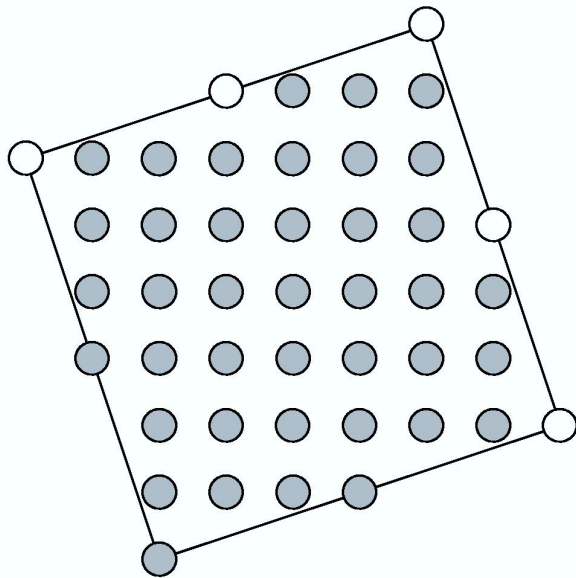


- Bravais lattice: translation vectors \mathbf{T}_1 , \mathbf{T}_2 (2D)



- finite lattices: finite multiples of \mathbf{T}_1 , \mathbf{T}_2 and boundary conditions
 - periodic, antiperiodic
 - open
- lattice symmetries:
 - translation – multiples of Bravais lattice vector + periodic (AP) BCs
 - rotations – e.g., $\pi/2$ for a square lattice (group C_{4v})
 - reflection – about symmetry axis

Tilted clusters



40-site cluster, square lattice ($a = 1$)

$$\mathbf{T}_1 = (1, 0), \quad \mathbf{T}_2 = (0, 1)$$

Spanning vectors:

$$\mathbf{F}_1 = (6, 2), \quad \mathbf{F}_2 = (-2, 6)$$

In general,

$$\mathbf{F}_1 = (n, m), \quad \mathbf{F}_2 = (-m, n)$$

$$N = n^2 + m^2$$

translational symmetry satisfied

\Rightarrow reflection/rotation symmetries become more complicated

I (ii) Representation of Many-Body States

mapping to (binary) integers:

- spin-1/2 Heisenberg:

$$|\uparrow_1 \downarrow_2 \dots \uparrow_{N-1} \uparrow_N\rangle \rightarrow 1_1 0_2 \dots 1_{N-1} 1_N$$

spin flip = bit flip

- Hubbard

$$|N_\ell^\uparrow N_\ell^\downarrow\rangle \rightarrow N_\ell^\uparrow N_\ell^\downarrow \quad \text{or} \quad |N_\ell^e S_\ell^z\rangle$$

with $N_\sigma = \{0, 1\}$

- other models (t - J , $S = 1$ Heisenberg, ...) more complicated

Symmetries: given group \mathcal{G} with generators $\{g_p\}$

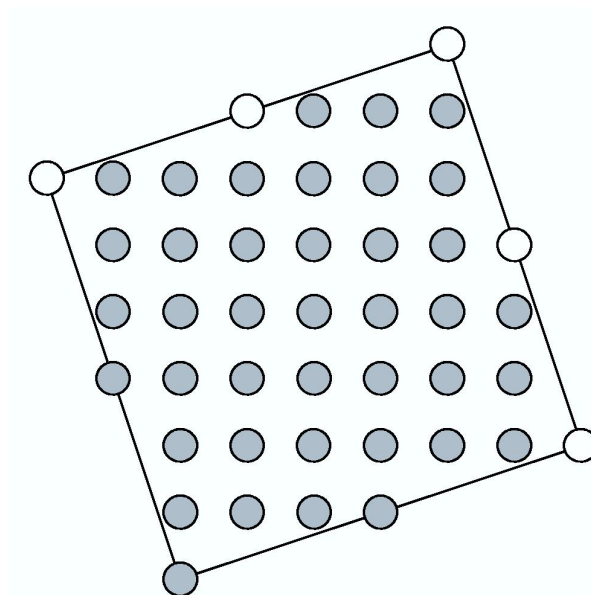
$$[H, g_p] = 0 \rightarrow H \text{ block diagonal (Hilbert space can be divided)}$$

- Continuous
 - conservation of particle number, S^z – $U(1) \Rightarrow$ permutations of bits
 - total spin $SU(2)$ difficult to combine with space group
 - \Rightarrow spin inversion (Z_2) can be used
- Space group
 - translation: abelian local states
 - point group (reflections and rotations): non-abelian in general

\Rightarrow form symmetrized linear combination of local states

Example

Reduction of Hilbert space for $S = 1/2$ Heisenberg on $\sqrt{40} \times \sqrt{40}$ cluster



- full Hilbert space: $\dim = 2^{40} = 10^{12}$
- constrain to $S_z = 0$: $\dim = 138 \times 10^9$
- using spin inversion: $\dim = 69 \times 10^9$
- utilizing all 40 translations: $\dim = 1.7 \times 10^9$
- using all 4 rotations: $\dim = 430,909,650$

I (iii) Complete Diagonalization

To solve $H |\psi\rangle = E |\psi\rangle$ (H real, symmetric)

Method (*Numerical Recipes*, Ch. 11)

1. Householder transformation - reduction to tridiagonal form T
 - $\approx 2n^3/3$ operations ($4n^3/3$ with eigenvectors)
2. Diagonalization of a tridiagonal matrix
 - roots of secular equation: inefficient
 - QL (QR) algorithm - factorization $T = Q L$,
 Q orthogonal, L lower triangular
 $\approx 30n^2$ operations ($\approx 3n^3$ with eigenvectors)

Useful for:

- Simple problems, testing
- Matrix H dense
- Many eigenstates required

But

- H must be stored
- entire matrix must be diagonalized

I (iv) Iterative Diagonalization

Idea: project H onto a cleverly chosen subspace of dimension $M \ll N$
 \Rightarrow good convergence of extremal eigenstates

Methods

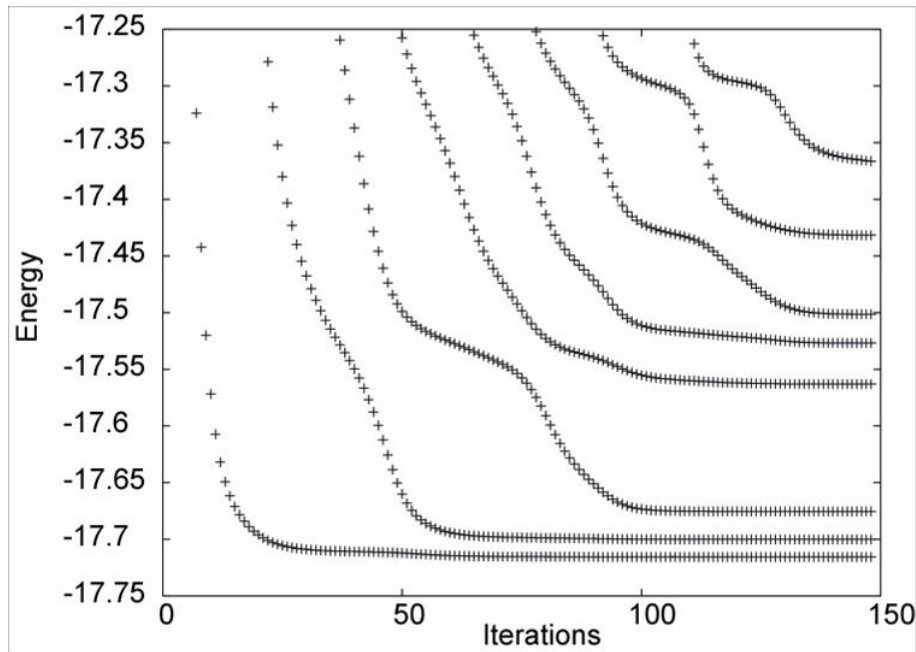
- Power method $|v_n\rangle = H^n|v_0\rangle$
 - conceptually simple, but converges poorly
 - needs only two vectors, $|v_n\rangle$ & $|v_{n-1}\rangle$
- Lanczos: orthogonal vectors in Krylov subspace (spanned by $\{|v_n\rangle\}$)
 - simple to implement
 - memory efficient - only 3 vectors needed at once
 - works well for sparse, short-range H
- Davidson: subspace expanded by diagonal approximation to inverse iteration
 - higher-order convergence than Lanczos (usually)
 - implementation more complicated
 - works best for diagonally-dominated H
- Jacobi-Davidson: generalization of Davidson
 - nontrivial problem-specific preconditioner (approximation to inverse)
 - can be applied to generalized eigenvalue problem

$$A|x\rangle = \lambda B|x\rangle \quad (A, B \text{ general, complex matrices})$$

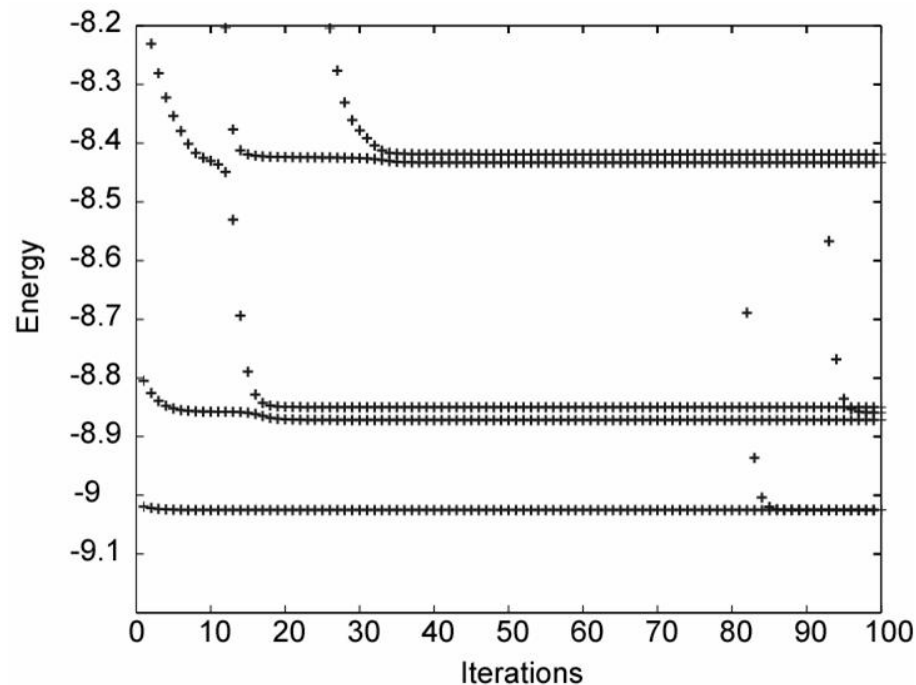
Lanczos Algorithm

- 0) choose $|u_0\rangle$ (random vector, $|\tilde{\psi}_0\rangle$ from last iteration, ...)
- 1) form $|u_{n+1}\rangle = H |u_n\rangle - a_n |u_n\rangle - b_n^2 |u_{n-1}\rangle$
where $a_n = \frac{\langle u_n | H | u_n \rangle}{\langle u_n | u_n \rangle}$ and $b_n^2 = \frac{\langle u_n | u_n \rangle}{\langle u_{n-1} | u_{n-1} \rangle}$
- 2) Is $\langle u_{n+1} | u_{n+1} \rangle < \varepsilon$?
yes: do 4) then stop
no: continue
- 3) repeat starting with 1) until $n = M$ (maximum dimension)
- 4) diagonalize $\langle u_i | H | u_j \rangle$ (tridiagonal) using QL algorithm
diagonal elements $\mathbf{D} = (a_0, a_1, \dots, a_n)$,
off-diagonal elements $\mathbf{O} = (b_1, b_2, \dots, b_n)$
 \Rightarrow eigenvalue \tilde{E}_0 , eigenvector $|\tilde{\psi}_0\rangle$
- 5) repeat starting with 0), setting $|u_0\rangle = |\tilde{\psi}_0\rangle$

Convergence of Lanczos Algorithm



- eigenvalues converge starting with extremal ones
- excited states can get “stuck” for a while

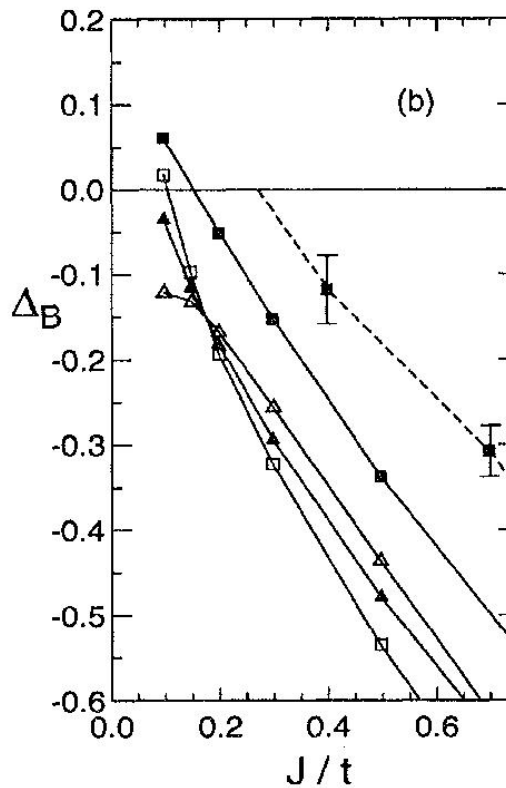
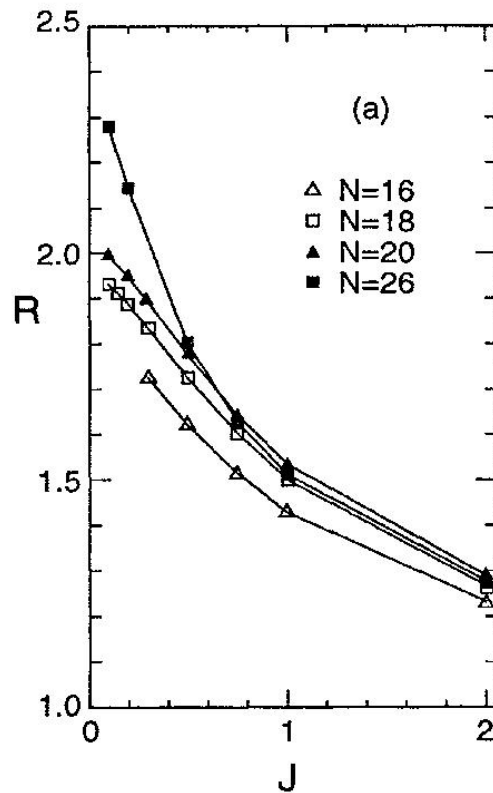


at longer times:

- true eigenvalues converged
- spurious or “ghost” eigenvalues produced
- multiplicity of eigenstates increases

Example: 2D t - J Model

Binding of 2 holes



R : average hole-hole distance
 Δ_B : binding energy

(Poiblan, Riera, & Dagotto, 1993)

- holes closer than two lattice spacings
- pair binding for $J > J_c$, but large finite-size effects

\Rightarrow Does binding persist for larger lattices and constant doping (more holes)?

I (v) Dynamics with Exact Diagonalization

Time-dependent correlation functions

$$C(t) = -i \langle \psi_0 | A(t) A^\dagger(0) | \psi_0 \rangle$$

Fourier transform to frequency space (retarded)

$$\tilde{C}(\omega + i\eta) = \langle \psi_0 | A (\omega + i\eta - H + E_0)^{-1} A^\dagger | \psi_0 \rangle \quad (\text{resolvent})$$

Spectral function

$$I(\omega) = -\frac{1}{\pi} \lim_{\eta \rightarrow 0^+} \text{Im} \tilde{C}(\omega + i\eta)$$

Examples from theory and experiment

name	notation	operators	experiment
single-particle spectral weight	$A(\mathbf{k}, \omega)$	$A = c_{\mathbf{k}, \sigma}$	photoemission
structure factor	$S_{zz}(\mathbf{q}, \omega)$	$A = S_{\mathbf{q}}^z$	neutron scattering
optical conductivity	$\sigma_{xx}(\omega)$	$A = j_x$	optics
4-spin correlation	$R(\omega)$	$\sum_{\mathbf{k}} R_{\mathbf{k}} \mathbf{S}_{\mathbf{k}} \cdot \mathbf{S}_{-\mathbf{k}}$	Raman scattering

Methods

Krylov space method (continued fraction)

restart Lanczos procedure with

$$|u_0\rangle = \frac{1}{\sqrt{\langle \psi_0 | A A^\dagger | \psi_0 \rangle}} A^\dagger |\psi_0\rangle$$

In this Lanczos basis,

$$\tilde{C}(z = \omega + i\eta + E_0) = \frac{\langle \psi_0 | A A^\dagger | \psi_0 \rangle}{z - a_1 - \frac{b_2^2}{z - a_2 - \frac{b_3^2}{z - a_3 - \dots}}}$$

Interpretation:

- calculation of eigenvector not needed
- consider Lehmann representation of spectral function

$$I(\omega) = \sum_n |\langle \psi_n | A^\dagger | \psi_0 \rangle|^2 \delta(\omega - E_n + E_0)$$

- \Rightarrow poles and weights of $\tilde{C}(z)$ determine $I(\omega)$
- weight decreases with $n \rightarrow$ truncate after M steps
- spectrum discrete \rightarrow finite broadening η

Correction vector method

(Soos & Ramasesha, 1984)

Calculate vectors

$$|\phi_0\rangle = A^\dagger |\psi_0\rangle, \quad |\phi_1\rangle = (\omega + i\eta - H + E_0)^{-1} |\phi_0\rangle$$

directly, then

$$I(\omega) = \frac{1}{\pi} \text{Im} \langle \phi_0 | \phi_1 \rangle$$

Advantages:

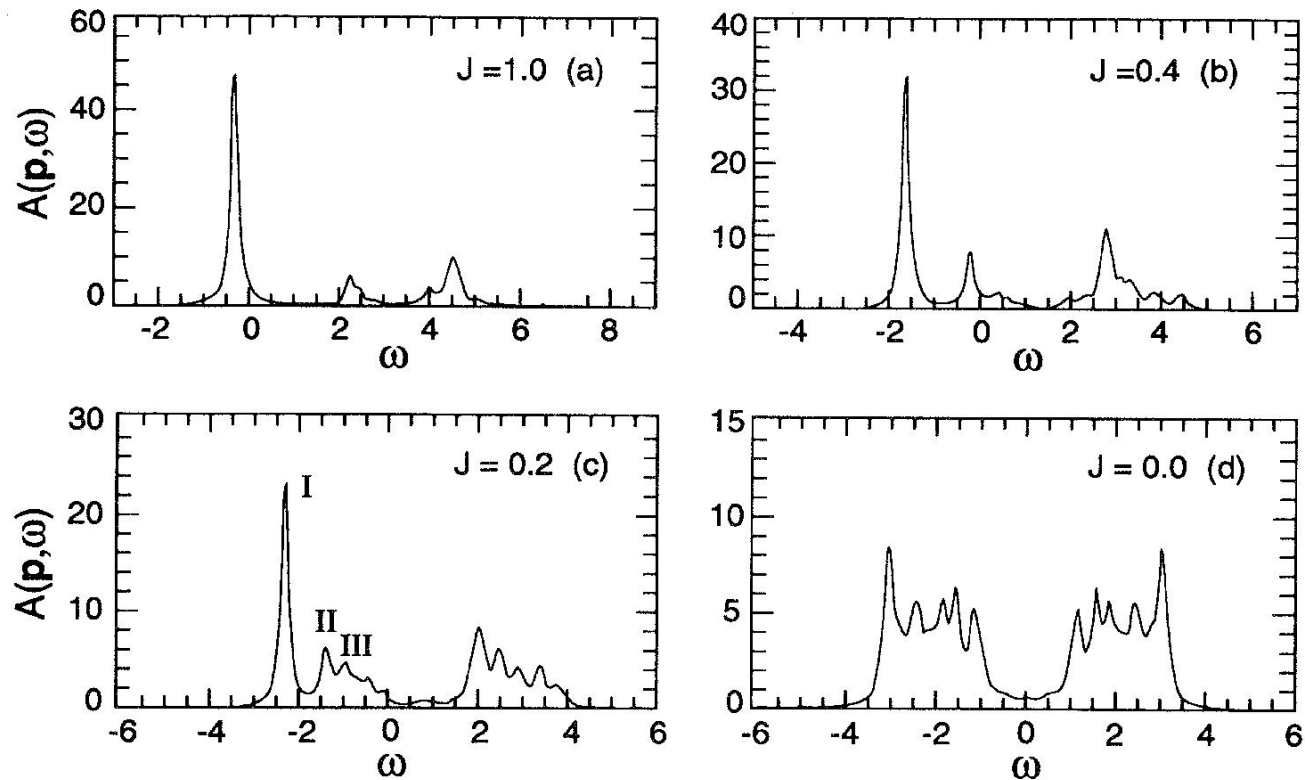
- spectral weight calculated exactly for a given range
- nonlinear spectral functions computed by higher order correction vectors
- can be run in conjunction with Davidson algorithm

Disadvantage: system $(H - z)|\phi_1\rangle = |\phi_0\rangle$ must be solved for each ω desired

Example: Dynamics in 2D t - J Model

Single-particle spectral weight $A(\mathbf{k}, \omega)$ at $\mathbf{k} = \mathbf{k}_F = (\pi/2, \pi/2)$ for one hole

4×4 lattice (Dagotto, Joynt, Moreo, Bacci, & Gagliano, 1993)



Does a single quasiparticle propagate in an antiferromagnet?

- strongly localized hole with string excitations at $J/t = 1.0$
- quasiparticle peak remains until $J/t = 0.4$
- “lump” with pseudogap at $J/t = 0.2$
- pseudogap due to finite-size effects at $J/t = 0$ (symmetric in ω)

I (vi) Finite Temperature with Exact Diagonalization

To calculate finite- T properties in orthonormal basis $|n\rangle$

$$\langle A \rangle = \frac{1}{Z} \sum_n \langle n | A e^{-\beta H} | n \rangle, \quad Z = \sum_n \langle n | e^{-\beta H} | n \rangle,$$

Problem: expensive to calculate for all $|n\rangle$

Idea: stochastic sampling of Krylov space (Jaklic & Prelovsek, 1994)

$$\langle A \rangle \approx \frac{1}{Z} \sum_s \frac{N_s}{R} \sum_r \sum_m e^{-\beta \epsilon_m^{(r)}} \langle r | \Psi_m^{(r)} \rangle \langle \Psi_m^{(r)} | A | r \rangle$$

where

$$Z \approx \sum_s \frac{N_s}{R} \sum_r \sum_m e^{-\beta \epsilon_m^{(r)}} \left| \langle r | \Psi_m^{(r)} \rangle \right|^2$$

- \sum_s over symmetry sectors of dimension N_s
- \sum_r average over R random starting vectors $|\Psi_0^{(r)}\rangle$
- \sum_m Lanczos propagation of starting vectors: $|\Psi_m^{(r)}\rangle$ at step m

\Rightarrow useful if convergence good when $M \ll N_s$ and $R \ll N_s$

Properties

- related to high- T expansion – $T \rightarrow \infty$ limit correct
- high to medium T properties in thermodynamic limit
- low-temperature limit correct (on finite lattice), up to sampling error
reduction of (large) sampling error: (Aichhorn *et al.*, 2003)

start with:

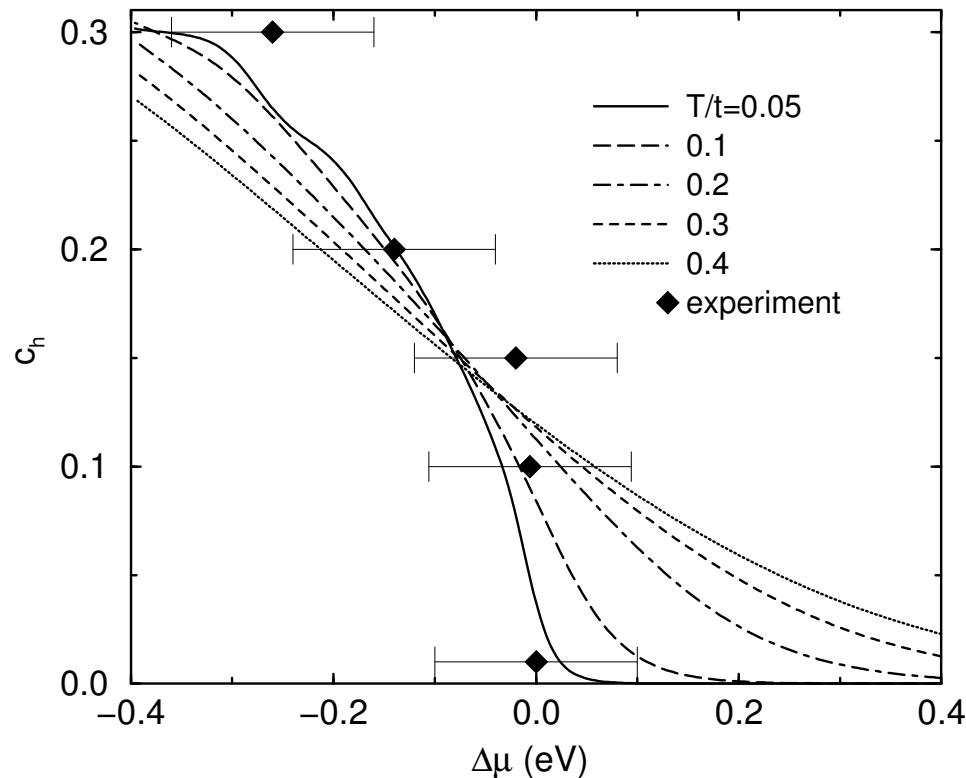
$$\langle A \rangle = \frac{1}{Z} \sum_n^N \langle n | e^{-\beta H/2} A e^{-\beta H/2} | n \rangle ,$$

\Rightarrow twofold insertion of Lanczos basis \rightarrow smaller fluctuations at low T

- can calculate
 - thermodynamic properties: specific heat, entropy, static susceptibility, ...
 - static correlation functions
 - dynamics: $A(\mathbf{k}, \omega)$, $S_{zz}(\mathbf{q}, \omega)$, $\sigma_{xx}(\omega)$, ...

Example: t - J Model at finite T

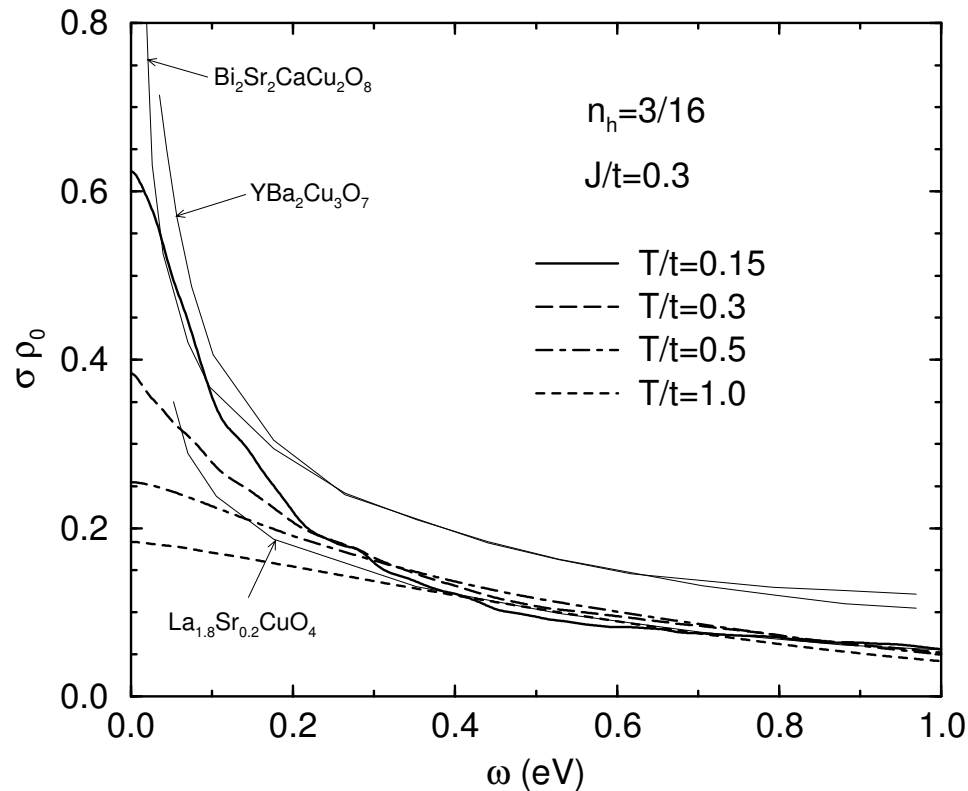
Hole concentration $c_h(=x)$ vs. chemical potential shift $\Delta\mu = \mu_h - \mu_h^0$
2D t - J model, 16, 18, 20 sites, $t/J = 0.3$, $t = 0.4\text{eV}$



(Jaklic & Prelovsek, 1998)

- experimental results for LSCO from photoemission shift (Ino *et al.*, 1997)
- holes only when $\mu < \mu_h^0 \approx -1.99t$ as $T \rightarrow 0$
- compressibility finite \Rightarrow no phase separation

Optical conductivity compared with various cuprates at intermediate doping



(Jaklic & Prelovsek, 1998)

- Cuprates measured at $T < 200\text{K}$, c_h somewhat uncertain
- high- T falloff slower for materials – transitions to higher excited states?
- experimental curves:
 - LCSO, $c_h \sim x = 0.2$ (Uchida *et al.*, 1991)
 - BISCCO, $c_h \sim 0.23$ (Romero *et al.*, 1992)
 - YBCO, $c_h \sim 0.23$ (Battlogg *et al.*, 1994)

Discussion: Exact Diagonalization

- Method conceptually straightforward, numerically exact
 - Iterative diagonalization allows the treatment of surprisingly large matrices
 - Efficient implementation using symmetries useful
 - System sizes nevertheless strongly restricted
 - Extensions to basic method can calculate
 - dynamical correlation functions
 - finite temperature properties
 - Not mentioned here, but also possible:
calculation of full time evolution of quantum state with Lanczos
- ⇒ Benchmark for other methods, useful when other methods fail

II (i) Anderson and Kondo Problem

Problem: one localized impurity in a noninteracting electron gas

Single Impurity Anderson Model (SIAM)

$$H^{AI} = \varepsilon_d n_\ell^d + U n_{\ell,\downarrow}^d n_{\ell,\downarrow}^d + \sum_{\mathbf{k},\sigma} \left(V_{\mathbf{k},d} c_{\mathbf{k},\sigma}^\dagger d_{\mathbf{k},\sigma} + \text{H.c.} \right) + \sum_{\mathbf{k},\sigma} \varepsilon_{\mathbf{k}} c_{\mathbf{k},\sigma}^\dagger c_{\mathbf{k},\sigma}$$

- general scattering $V_{\mathbf{k},d}$ between impurity and band
- Coulomb interaction on d -site only
- usual simplifications:
 - isotropic scattering: $V_{\mathbf{k},d} \Rightarrow V_{k,d}$, $c_{\mathbf{k},\sigma} \Rightarrow c_{k,l=m=0,\sigma}$ (s-wave)
 - symmetric: $\varepsilon_d = -U/2$
 - constant or semi-elliptical density of states

Mapping onto semi-infinite chain

$$\begin{aligned} \tilde{H}^{AI} = & \varepsilon_d n_\ell^d + U n_{\ell,\downarrow}^d n_{\ell,\downarrow}^d + V \sum_{\mathbf{k},\sigma} \left(f_{0,\sigma}^\dagger d_\sigma + \text{H.c.} \right) \\ & + \sum_{n=0,\sigma}^{\infty} \left[\varepsilon_n f_{n,\sigma}^\dagger f_{n,\sigma} + \lambda_n \left(f_{n,\sigma}^\dagger f_{n+1,\sigma} + \text{H.c.} \right) \right] \end{aligned}$$

obtained through Lanczos tridiagonalization of $\sum_{\mathbf{k},\sigma} \varepsilon_{\mathbf{k}} c_{\mathbf{k},\sigma}^\dagger c_{\mathbf{k},\sigma}$

where $V f_{0,\sigma}^\dagger = \sum_{\mathbf{k}} V_{k,d} c_{\mathbf{k},\sigma}^\dagger$ and $V^2 = \sum_{\mathbf{k}} |V_{k,d}|^2$

Kondo model

$$H^K = J_K \mathbf{S}_d \cdot \mathbf{s}_0 + \sum_{\mathbf{k}, \sigma} \epsilon_{\mathbf{k}} c_{\mathbf{k}, \sigma}^\dagger c_{\mathbf{k}, \sigma} \quad \text{with} \quad \mathbf{s}_0 = f_{0, \sigma}^\dagger \vec{\sigma}_{\sigma \mu} f_{0, \mu}, \quad f_{0, \sigma} = \sum_{\mathbf{k}} c_{\mathbf{k}, \sigma}$$

- strong-coupling limit ($U \gg V^2$) of symmetric, isotropic H^{AI} (Schrieffer-Wolff transformation)
- local, isotropic coupling of spin to band

Mapping to a linear chain model via

1. Lanczos tridiagonalization
2. constant density of states ρ_0
3. logarithmic discretization of conduction band

$$\tilde{H}^K = \frac{1}{2}(1 + \Lambda^{-1}) \sum_{n=0}^{\infty} \Lambda^{-n/2} \left(f_{n, \sigma}^\dagger f_{n+1, \sigma} + \text{H.c.} \right) + 2J_K \rho_0 f_{0, \sigma}^\dagger \vec{\sigma}_{\sigma \mu} f_{0, \mu}$$

where the Lanczos coefficients $\epsilon_n = 0$ and $\lambda_n \approx \frac{1}{2}(1 + \Lambda^{-1})\Lambda^{-n/2}$, $n \gg 1$

\Rightarrow “hopping” falls off exponentially!

Related models

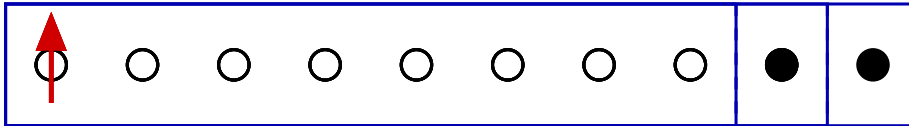
- anisotropic Kondo model $\mathbf{S}_d \cdot \mathbf{s}_0 \rightarrow S_d^z s_0^z + \frac{\alpha}{2}(S_d^+ s_0^- + S_d^- s_0^+)$
- Ohmic two-state system
- generalized Anderson impurity model (DMFT)

II (ii) Numerical Renormalization Group for Kondo Problem

(Wilson, 1974)

Idea: Numerically integrate out degrees of freedom \rightarrow low-energy properties

Kondo problem \rightarrow 1D quantum lattice model (4^N degrees of freedom)



- isolate finite system
- diagonalize numerically
- keep m lowest energy eigenstates
- add a site
- iterate

Assumption: low-energy states most important for low-energy behavior of larger system

\Rightarrow powerful method for impurity problems (Kondo, Anderson, ...)

Why does it work so well?

- Each system size corresponds to a lower energy scale
- Each RG step can be justified perturbatively (Λ^{-1} is a small parameter)
- substantial portion ($1/4$) of Hilbert space is kept at each step

Calculation of observables with the NRG

Effective Hamiltonian for a given size associate with energy scale

$$\bar{H}_N \equiv H_N/D_N \quad , \quad D_N = \frac{1}{2}(1 + \Lambda^{-1}) \Lambda^{-(N-1)/2} \quad (\text{lowest scale})$$

- RG flow - fixed point defined by $R[H^*] = H^*$
numerically: range $N_1 \leq N \leq N_2$ in which $\bar{E}_p^N \approx \bar{E}_p$ (independent of N)
 \Rightarrow identify fixed points and crossover energy scales
- thermodynamic quantities

effective partition function at scale D_N

$$Z_N(T) \equiv \text{Tr} e^{-H_N/k_B T} = \sum_p e^{-E_p^N/k_B T}$$

valid at $k_B T = k_B T_N \approx D_N$

other quantities can be formed from the partition function

e.g., impurity susceptibility for Anderson model

$$\chi_{\text{imp}}(T) = \frac{(g\mu_B)^2}{k_B T} \left[\frac{1}{Z} \text{Tr}(S_z^{\text{tot}})^2 e^{-H/k_B T} - \frac{1}{Z_c} \text{Tr}(S_{z,c}^{\text{tot}})^2 e^{-H_c/k_B T} \right]$$

- dynamical quantities ($T = 0$)
e.g., impurity spectral function:

$$A(\omega) = -\frac{1}{\pi} \text{Im} G(\omega + i\eta) \quad \text{where } G(t) = -i \langle \psi_0 | T d(t) d^\dagger(0) | \psi_0 \rangle$$

At finite N ,

$$A_N(\omega) = \frac{1}{Z_N} \sum_p |\langle p | d_\sigma^\dagger | 0 \rangle|^2 \delta(\omega - E_p + E_0) + |\langle 0 | d_\sigma^\dagger | p \rangle|^2 \delta(\omega + E_p - E_0)$$

$$A_N(\omega) \approx A(\omega) \text{ when } \omega \approx \omega_N \equiv k_B T_N$$

\Rightarrow dynamics can be performed at the current RG energy scale

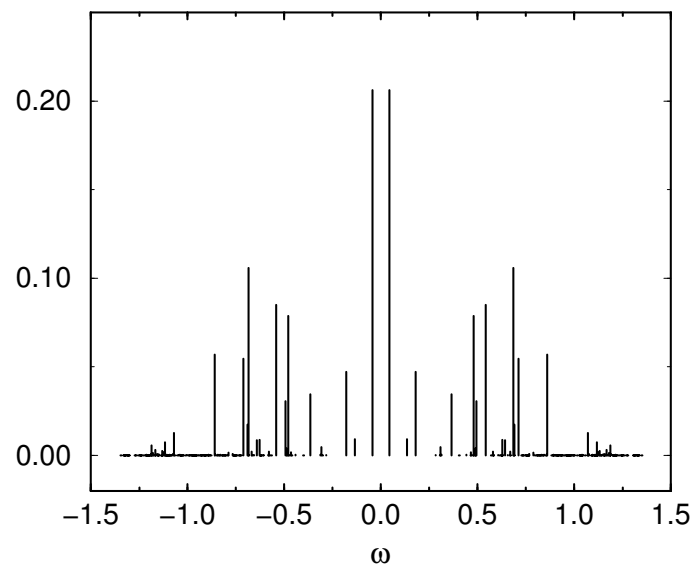
- energy summation gives sum of δ -functions
- broadening needed to get a continuous spectrum
- dynamical properties at finite- T similar (appropriate T , ω)
 \Rightarrow transport properties

Dynamics at finite N

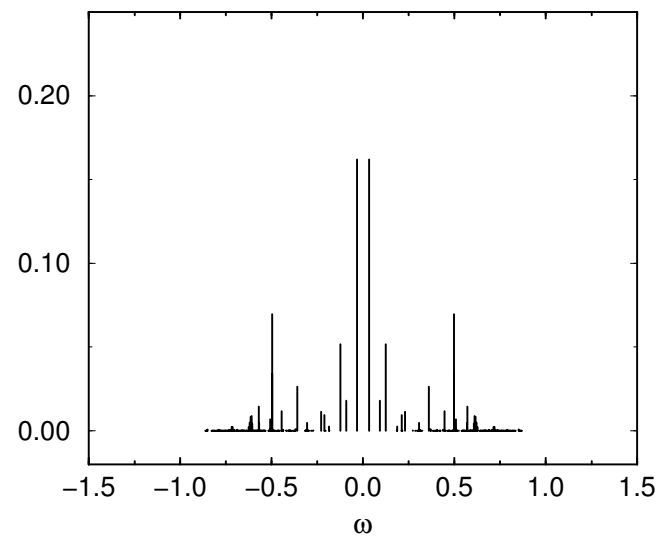
(SIAM)

(Bulla, 2000)

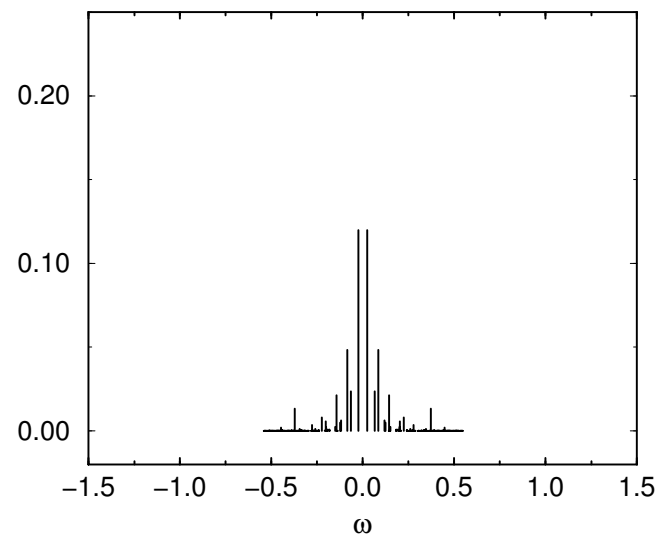
$N = 14$



$N = 16$



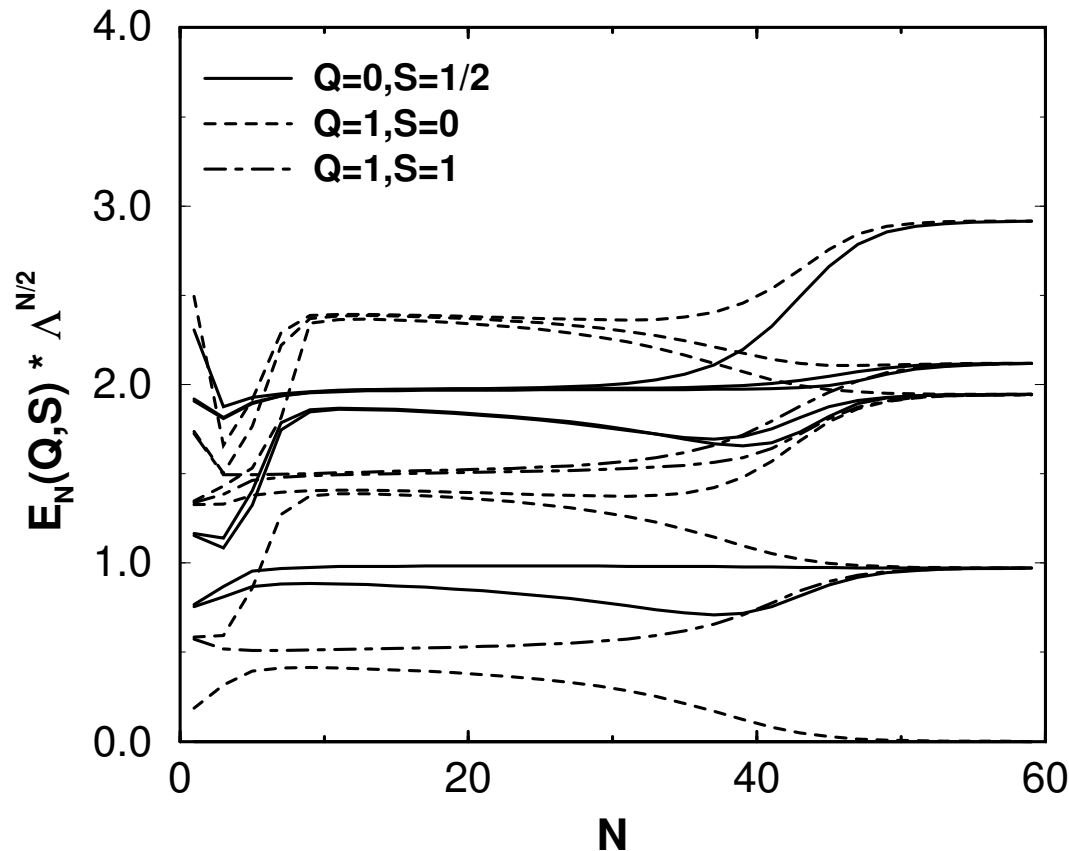
$N = 18$



Physics of the Kondo Problem

Flow of coupling constants

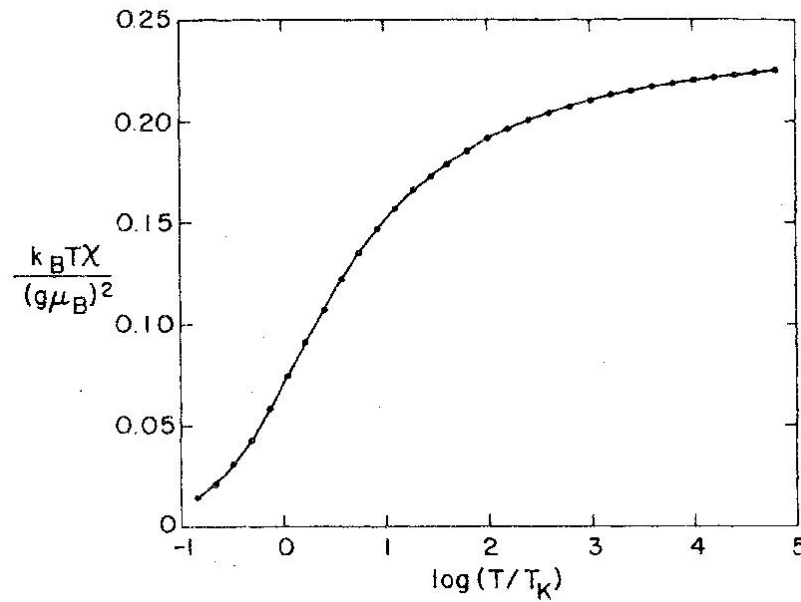
(SIAM, $\varepsilon_d = -0.2$, $U = 0.4$, $\Delta = \frac{1}{2}\pi V^2 N(E_f) = 0.015$)



(Bulla, 2000)

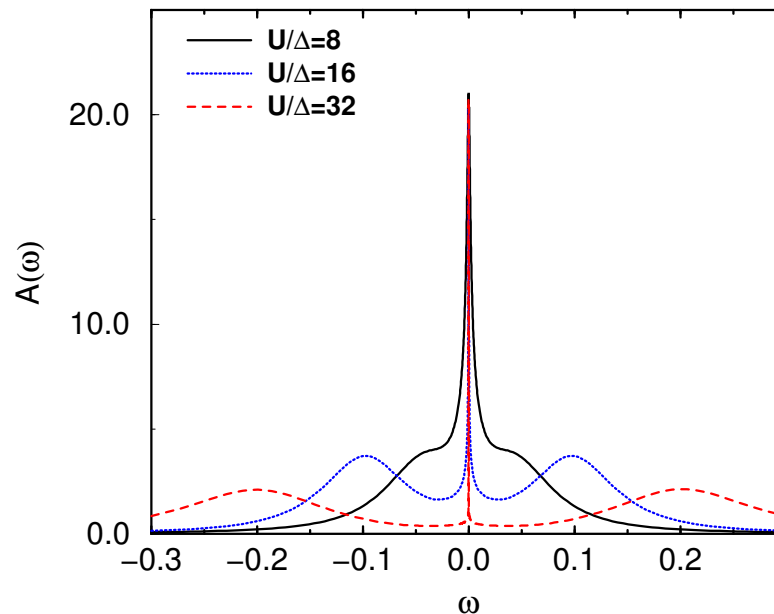
- Crossover to local moment behavior at $N \approx 5 \Rightarrow$ unstable fixed point
- Crossover to screening behavior at energy scale $k_B T_K \Rightarrow$ stable low- T fixed point

Susceptibility universal on Kondo scale \Rightarrow universal value at $T = 0$



(Krishna-murthy, Wilkins,
& Wilson, 1980)

Quasiparticle peak at Fermi energy in SIAM



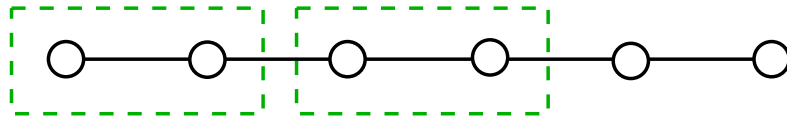
(Bulla, 2000)

Application to other quantum lattice models unsuccessful:

- 1D Hubbard model (Bray & Chui, 1979)
lattice size $L = 2, 4, 8, 16$
10% error in E_0 after 4 steps $\Rightarrow L = 16$
 - 1D Heisenberg model (Xiang & Gehring, 1992)
 $S = 1$, $L = 18$ sites, OBCs: 3% error in E_0
 - 2D Anderson localization (Lee, 1979)
Found a localization transition in 2D
(scaling theory: no transition, 2D critical dimension)
- \Rightarrow separation of energy scales not applicable

Single-Particle Problem

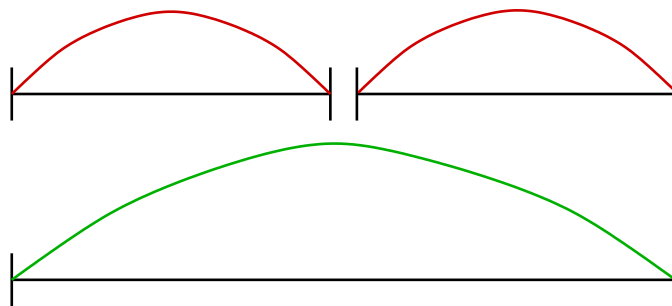
Wilson procedure for particle on a tight-binding lattice (Wilson, 1985)



$$H = \left(\begin{array}{cc|cc} 2 & -1 & 0 & 0 \\ -1 & 2 & -1 & 0 \\ \hline 0 & -1 & 2 & -1 \\ 0 & 0 & -1 & 2 \end{array} \right) \rightarrow -\frac{\partial^2}{\partial x^2} + \text{fixed BCs}$$

(equivalent to modes of a string with fixed ends)

Putting two “blocks” together



⇒ treatment of boundaries critical

	<u>State</u>	<u>Exact</u>	<u>NRG</u>	
Test calculation:	E_0	2.351×10^{-6}	1.9207×10^{-2}	10 blockings (2048 sites)
	E_1	9.403×10^{-6}	1.9209×10^{-2}	
	E_2	2.116×10^{-5}	1.9714×10^{-2}	

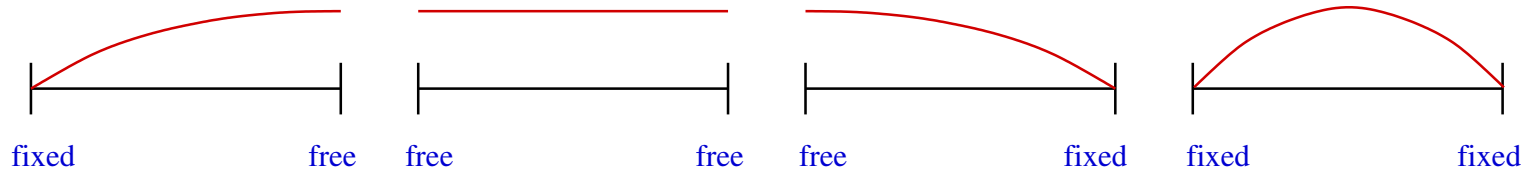
Discussion: Numerical RG

- Iterative diagonalization scheme - effort per step remains constant as system grows
 - Truncation carried out by transforming to the basis of m lowest energy eigenstates
 - Degrees of freedom added by adding site
 - NRG works well for impurity problems because of exponential separation of energy scales on effective chain model
 - Thermodynamics, dynamical correlations, and transport properties can be calculated
 - NRG becomes inaccurate quickly for quantum lattice models such as Hubbard and Heisenberg chains
 - Origin of problem can be understood for single particle on a tight-binding chain – treatment of boundaries as blocks are put together
- ⇒ Very useful for the right problem, but can fail badly

III (i) Better Methods for the Noninteracting Particle

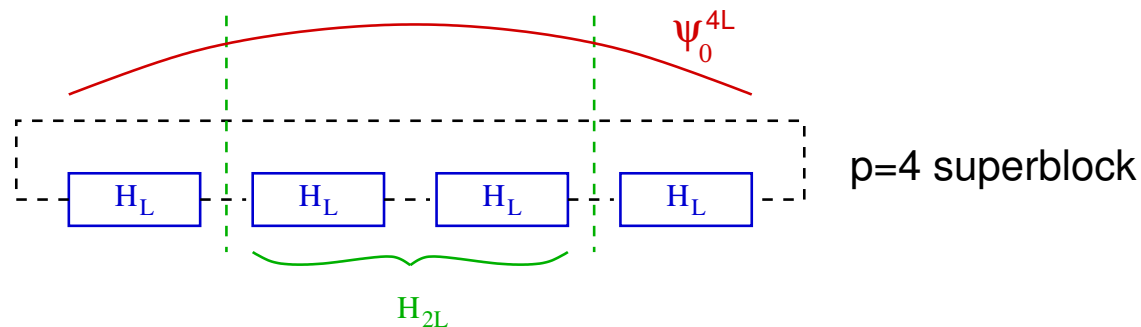
Combinations of BCs technique

(White & Noack, 1992)



- Diagonalize H_L with different combinations of BCs
 - Use orthogonalized set of states as new basis
 - Energies accurate to 10 digits (2 states/BC, 10 iterations)
- ⇒ Not easy to generalize to interacting systems

Superblock technique



Idea: Fluctuations in additional blocks allow general behavior at boundaries

- Diagonalize superblock of p blocks
 - Project wavefunctions onto size $2L$ block, orthogonalize
 - Exact as $p \rightarrow \infty$
- ⇒ Projection is no longer trivial for interacting systems

Review: entanglement in quantum mechanics

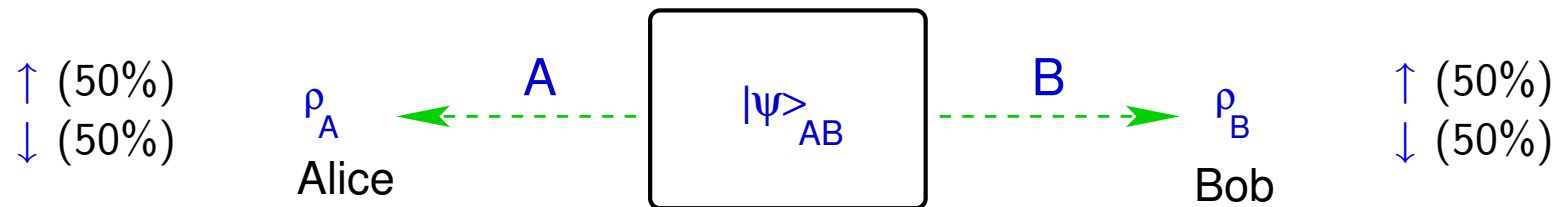
system made up of $S = \frac{1}{2}$ spins A, B

$$|\uparrow\uparrow\rangle \equiv |\uparrow\rangle_A \otimes |\uparrow\rangle_B \quad (\text{or } |\downarrow\downarrow\rangle, |\uparrow\downarrow\rangle, |\downarrow\uparrow\rangle)$$

superposition:

$$|\psi\rangle = \frac{1}{\sqrt{2}} (|\uparrow\uparrow\rangle + |\downarrow\downarrow\rangle)$$

Measurements:



measurements correlated: $A \uparrow \Rightarrow B \uparrow$ with 100% probability

\Rightarrow state (maximally) entangled!

Einstein, Podolsky, Rosen (1935): “spooky action-at-a-distance”
(spukhafte Fernwirkung)

Schrödinger (1935): entanglement *essential* property of quantum mechanics!

More complete description: density matrices

density matrix describes part of system

$$\rho_A = \text{Tr}_B |\psi\rangle \langle\psi| = \begin{pmatrix} \frac{1}{2} & 0 \\ 0 & \frac{1}{2} \end{pmatrix} \quad (\text{similar for } \rho_B)$$

⇒ mixed state

Schmidt decomposition

$$|\psi\rangle_{AB} = \sum_{\alpha} \sqrt{w_{\alpha}} |\phi_{\alpha}\rangle_A |\chi_{\alpha}\rangle_B = \frac{1}{\sqrt{2}} (|\uparrow\uparrow\rangle + |\downarrow\downarrow\rangle)$$

$|\phi_{\alpha}\rangle_A$: eigenstate of ρ_A , $|\chi_{\alpha}\rangle_B$: eigenstate of ρ_B

w_{α} : common eigenvalues

Schmidt number: number of $w_{\alpha} \neq 0$

= 1: $|\psi\rangle = |\phi_0\rangle_A |\chi_0\rangle_B$ e.g., $= |\uparrow\uparrow\rangle$ not entangled

> 1: A and B entangled

Relationship to Quantum Information

relabeling:

$$|\downarrow\rangle \equiv |0\rangle, \quad |\uparrow\rangle \equiv |1\rangle \Rightarrow \text{qubit}$$

Is information contained in a pair of qubits?

quantum information content: von Neumann entropy

$$S(\rho) = -\text{Tr } \rho \log \rho$$

examples:

- $|\psi\rangle = |\phi\rangle|\chi\rangle$: $S(\rho_A) = 0 \Rightarrow$ classical
- $|\psi\rangle = \frac{1}{\sqrt{2}} (|1\rangle|1\rangle + |0\rangle|0\rangle)$: $S(\rho_A) = 1 \Rightarrow$ entangled qubits

entanglement: mutual quantum information

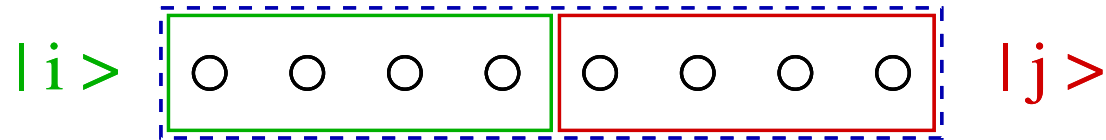
classical analog: Shannon entropy – information content in a message

Applications of entanglement

- quantum data compression
- quantum cryptography
- quantum teleportation
- quantum computing

III (ii) Density-Matrix Projection

What can be learned from dividing a many-body system?



- For the state $|\psi_0\rangle$ of the system (or approximation)
- reduced density matrix of subsystem (“system block”)

$$\rho = \text{Tr}_{|j\rangle} |\psi_0\rangle \langle \psi_0|$$

trace over states of the “environment block”

Properties:

- eigenstates $|\phi_\alpha\rangle$ form a complete basis for system block
- eigenvalues w_α
 - weight of a state
 - entanglement/mutual quantum information

$$S(\rho) = -\text{Tr}_{|j\rangle} (\rho \log \rho) = -\sum_\alpha w_\alpha \log w_\alpha$$

- optimal approximation: sum over m eigenstates with the largest w_α

$$|\psi_0\rangle \approx \sum_{\alpha}^{m < \dim(\alpha)} \sqrt{w_\alpha} |\phi_\alpha\rangle |\chi_\alpha\rangle \quad (\text{Schmidt decomposition})$$

Density Matrix Renormalization Group

(White, 1992)

Goal: ground-state properties of a 1D quantum lattice model

Density-matrix projection

- diagonalization (e.g., Lanczos) of a finite lattice $\Rightarrow |\psi_0\rangle$
- division of system
- reduction of the system block basis via density matrix $\Rightarrow m$ states
- Properties:
 - variational, ground state properties (numerically) on a finite lattice
 - very exact for 1D models with “open” boundary conditions
 - energies, local quantities most accurate
 - correlation functions (somewhat) less accurate

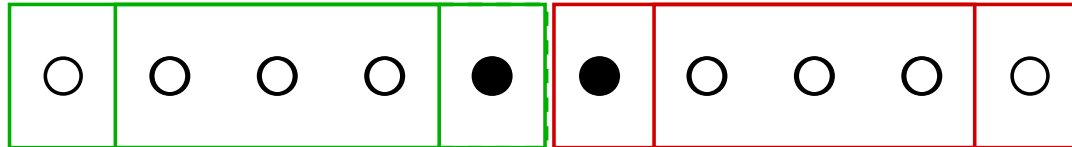
Buildup of system (RG)

- add one site at a time \Rightarrow fewest possible degrees of freedom at once
- need to choose environment block possibilities:
 - one or more “exact” sites
 - reflection of system block
 - stored block from a previous step

III (iv) DMRG Algorithms

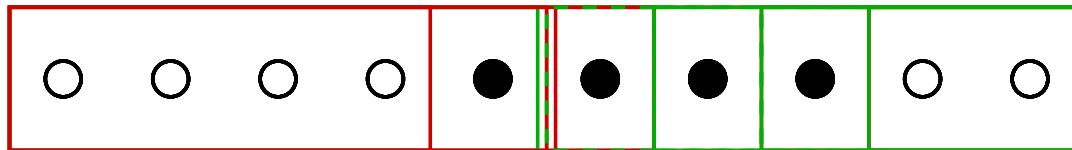
2 ways of building up superblock, depending on choice of the environment block

Infinite System Algorithm



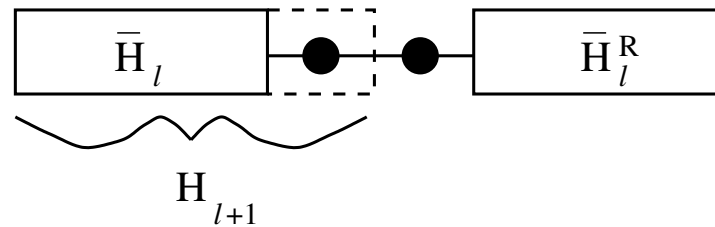
- environment block: reflection of the system block
- superblock grows by 2 lattice sites per iteration

Finite System Algorithm



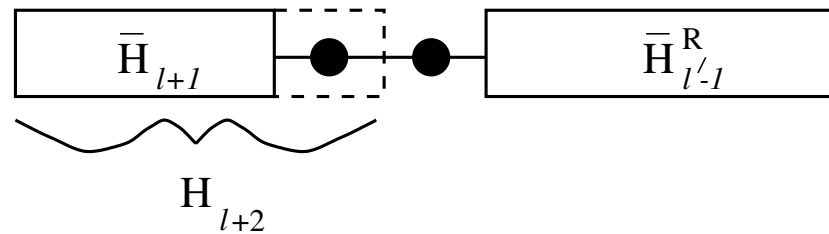
- starting point: infinite system method
- size of superblock stays the same environment block shrinks
- “zipping” back and forth \Rightarrow iterative convergence
- environment block stored from previous iteration

Infinite System Algorithm in Detail



1. Form a superblock containing L sites which is small enough to be exactly diagonalized.
2. Diagonalize the superblock Hamiltonian H_L^{super} numerically, obtaining *only* the ground state eigenvalue and eigenvector $|\psi\rangle$ using the Lanczos or Davidson algorithm.
3. Form the reduced density matrix $\rho_{ii'}$ for the new system block from $|\psi\rangle$ using $\rho_{ii'} = \sum_j \psi_{ij}^* \psi_{i'j}$. Note that $\ell' = \ell = L/2 - 1$.
4. Diagonalize $\rho_{ii'}$ with a dense matrix diagonalization routine to obtain the m eigenvectors with the largest eigenvalues.
5. Construct $H_{\ell+1}$ and other operators in the new system block and transform them to the reduced density matrix eigenbasis using $\bar{H}_{\ell+1} = O_L^\dagger H_{\ell+1} O_L$, $\bar{A}_{\ell+1} = O_L^\dagger A_{\ell+1} O_L$, etc., where the columns of O_L contain the m highest eigenvectors of $\rho_{ii'}$, and $A_{\ell+1}$ is an operator in the system block.
6. Form a superblock of size $L + 2$ using $\bar{H}_{\ell+1}$, two single sites and $\bar{H}_{\ell+1}^R$.
7. Repeat starting with step 2, substituting H_{L+2}^{super} for H_L^{super} .

Finite System Algorithm in Detail

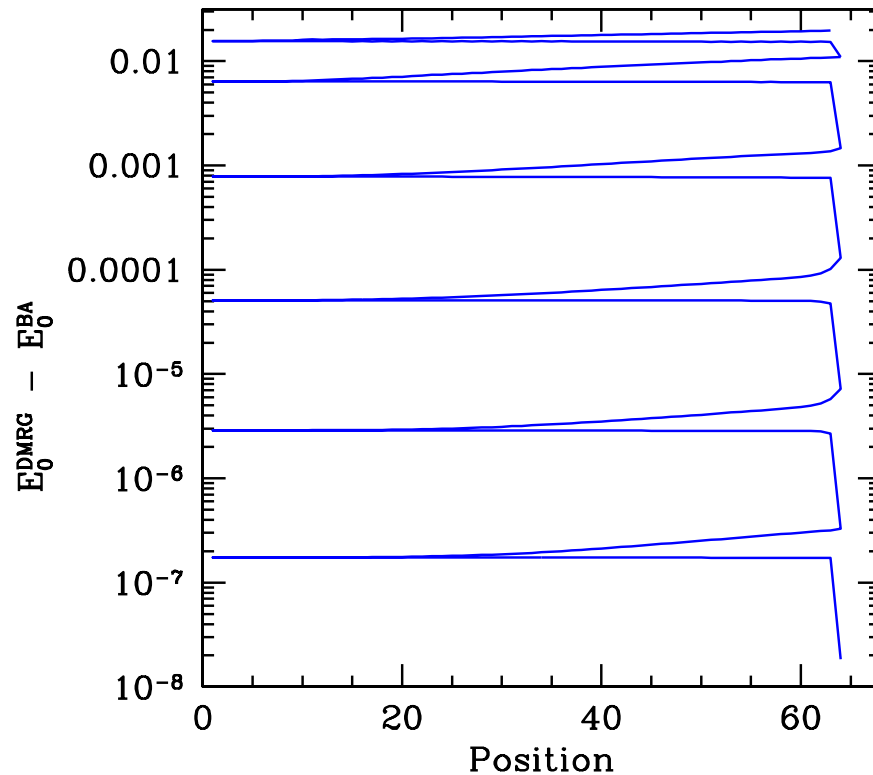


0. Carry out the infinite system algorithm until the superblock reaches size L , storing \bar{H}_ℓ and the operators needed to connect the blocks at each step.
1. Carry out steps 3-5 of the infinite system algorithm to obtain $\bar{H}_{\ell+1}$. Store it. (Now $\ell \neq \ell'$.)
2. Form a superblock of size L using $\bar{H}_{\ell+1}$, two single sites and $\bar{H}_{\ell'-1}^R$. The superblock configuration shown above where $\ell' = L - \ell - 2$.
3. Repeat steps 1-2 until $\ell = L - 3$ (i.e. $\ell' = 1$). This is the *left to right* phase of the algorithm.
4. Carry out steps 3-5 of the infinite system algorithm, reversing the roles of \bar{H}_ℓ and $\bar{H}_{\ell'}^R$, i.e. switch directions to build up the right block and obtain $\bar{H}_{\ell'+1}^R$. Store it.
5. Form a superblock of size L using $\bar{H}_{\ell-1}$, two single sites and $\bar{H}_{\ell'+1}^R$.
6. Repeat steps 4-5 until $\ell = 1$. This is the *right to left* phase of the algorithm.
7. Repeat starting with step 1.

Convergence of the DMRG

Comparison with exact solution (Bethe ansatz):
1D Hubbard model, 128 sites, open BCs

$L=128, t=1, U=4, \langle n \rangle=1$



- finite system algorithm, 6 iterations
- $m = 50$ to 800 states kept
- reflection symmetry at center used
- CPU time: ca. 6 hours on a 1.2 MHz Athlon

⇒ energy exact to 10 decimal places!

Applications: spin chains (XY, Heisenberg, biquadratic, $S = 1/2, 1, 3/2, 2, \dots$),
1D Hubbard-like models (plain, extended, ionic, Peierls-, ...)

What can be done with the DMRG?

What is it? Approximate diagonalization on a finite lattice

- Variational
- Large systems (up to 1000 sites)
- Accuracy comparable to exact diagonalization (in many cases)
- No problems with frustration or fermions
- What can be calculated?
 - Ground-state properties: gaps, correlation functions, susceptibilities
 - Dynamics of a quantum system
 - Finite temperature (high and low temperature)
 - Classical systems at finite temperature
 - Time evolution of a quantum system

Limitations

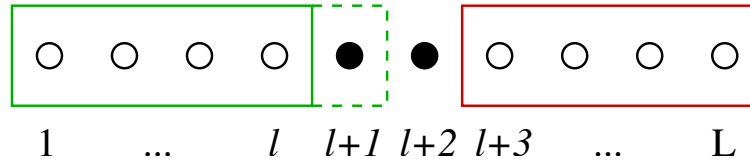
- Convergence depends on details of system
 - dimensionality (1D best)
 - boundary conditions (open BCs best)
 - range of Hamiltonian (short-range best)
- Efficient program can be complicated

Single-Particle Problem Revisited

More DMRG-like algorithm for single-particle problem

$$H_{ij} = 2 \delta_{ij} - \delta_{i,i+1} - \delta_{i,i-1}$$

Divide the system into 4 parts:



Use *one* basis state per block ($m = 1$) so that

$$\psi_j = \begin{cases} a_1 L_j & j \leq l \\ a_2 & j = l+1 \\ a_3 & j = l+2 \\ a_4 R_j & j \geq l+3 \end{cases}$$

Hamiltonian matrix element between ψ and ψ' :

$$\langle \psi | H | \psi' \rangle = \begin{pmatrix} a_1 \\ a_2 \\ a_3 \\ a_4 \end{pmatrix}^T \begin{pmatrix} H_{11} & T_{12} & 0 & 0 \\ T_{12} & 2 & -1 & 0 \\ 0 & -1 & 2 & T_{34} \\ 0 & 0 & T_{34} & H_{44} \end{pmatrix} \begin{pmatrix} a'_1 \\ a'_2 \\ a'_3 \\ a'_4 \end{pmatrix}$$

where

$$\begin{aligned} H_{11} &= \langle L | H | L \rangle, & H_{44} &= \langle R | H | R \rangle \\ T_{12} &= \langle L | H | l+1 \rangle = -L_\ell, & T_{34} &= \langle l+2 | H | R \rangle = -R_{\ell+3} \end{aligned}$$

Algorithm to find the ground state

Given $L(\ell)$ and $R(\ell + 3)$ – left and right bases at step ℓ

- Iteratively improve $\{L(\ell)\}$ by getting improved $L(\ell + 1)$, given $L(\ell)$ and $R(\ell + 3)$ (left to right)
- Then improve $\{R(\ell)\}$, given $L(\ell)$ and $R(\ell + 3)$ (right to left)

Basic left to right step

- Diagonalize H (4×4 matrix) to get ground state (a_1, a_2, a_3, a_4)
- Normalize a_1 and a_2 as $a'_1 = a_1/N$, $a'_2 = a_2/N$, $N = \sqrt{a_1^2 + a_2^2}$

- New basis state is then
$$L(\ell + 1)' = \begin{pmatrix} a'_1 L(\ell)_1 \\ \vdots \\ a'_1 L(\ell)_\ell \\ a'_2 \end{pmatrix}$$

- New Hamiltonian matrix element is

$$\langle L(\ell + 1)' | H | L(\ell + 1)' \rangle = a_1'^2 \langle L(\ell) | H | L(\ell) \rangle + 2a_2'^2 - 2a_1' a_2' L(\ell)_\ell$$

If $L(\ell)$ and $R(\ell + 3)$ were pieces of exact ground state, this would be exact
 \Rightarrow energy cannot increase.

Since we add degrees of freedom when $\ell \rightarrow \ell + 1$, energy will decrease if state is not exact ground state.

Initialization (infinite system procedure)

- Start with $L = 4$ to get $L(2)$
- Reflect $L(2)$ to get $R(5) \Rightarrow L = 6$
- Increase L by 2 until desired size is reached

Implementation in C++

(Uses “MatrixRef” matrix library by S.R.W. and R.M.N.)

C++ can use natural “objects” such as blocks:

(file pbox.h)

```
class Block
{
public:
    Real H11;
    Real L_inner;

    Block() // Default: construct a one-site block
        : H11(2.0), L_inner(1.0) { }
    Block Reflect() const { return *this; }
};
```

- `H11` and `L_inner` are real numbers containing H_{11} (H_{44}) and L_ℓ ($R_{\ell+3}$) for left (right) blocks
- `Block()` (the default constructor) defines that `Block S;` will create a block consisting of a single site
- `Reflect()` interchanges left and right blocks, i.e.
`Block R = L.Reflect();` (actually just returns itself)

Now define the collection of blocks making up the system:

```
class WaveFunction;

class System
{
public:
    const Block& b1;
    const Block& b2;
    const Block& b3;
    const Block& b4;

    System(const Block& bb1, const Block&bb2,
           const Block&bb3, const Block&bb4)
        : b1(bb1), b2(bb2), b3(bb3), b4(bb4) { }

    Real GetGroundState(WaveFunction& p);
};
```

- `b1`, `b2`, `b3`, `b4` are *references* to four blocks
- The statement
`System S(leftblock,siteblock,siteblock,rightblock);`
creates a system of four blocks
- `GetGroundState` returns the ground state energy and ground state wavefunction `p` (will be defined later, in “pbox.cc”)

Still need to define a WaveFunction:

```
class WaveFunction
{
public:
    Vector v;
    WaveFunction() : v(4) {}
};
```

just a vector of length 4, `Vector` is from MatrixRef library

Definition of GetGroundState: (file pbox.cc)

```
Real System::GetGroundState(WaveFunction& p)
{
  Matrix H(4,4), evecs(4,4);
  Vector evals(4);
  H = 0.0;
  H(1,1) = b1.H11;
  H(2,2) = b2.H11;
  H(3,3) = b3.H11;
  H(4,4) = b4.H11;
  H(1,2) = H(2,1) = -b1.L_inner;
  H(2,3) = H(3,2) = -1.0;
  H(3,4) = H(4,3) = -b4.L_inner;
  EigenValues(H,evals,evecs);
  p.v = evecs.Column(1);
  if(p.v.sumels() < 0.0) p.v *= -1.0;
  Real energy = evals(1);
  return energy;
}
```

- Forms the 4×4 matrix H as defined previously
- Diagonalizes H using `EigenValues` from `MatrixRef`
- Puts lowest eigenvector in `p`
- Return value is lowest eigenvalue

The density matrix for the noninteracting system involves just a_1 and a_2 (a_4 and a_3 for right block):

```
enum LR {Left, Right};
class DensityMatrix
{
public:
    Real a,b;
    DensityMatrix(const WaveFunction& psi,LR lr) {
        if(lr == Left)
            { a = psi.v(1); b = psi.v(2); }
        else
            { a = psi.v(4); b = psi.v(3); }
    }
    Vector NewBasis() {
        Vector res(2);
        Real norm = sqrt(a*a+b*b);
        res(1) = a / norm;
        res(2) = b / norm;
        return res;
    }
};
```

- An `enum` takes on a finite set of values, `LR`: left/right flag
- `NewBasis()` defines the new basis by normalizing `a`, `b`

This new basis can be used to form a new (left) block:

```
Block NewLeft(const Block& b1, const Block& b2, const Vector& bas)
{
    Block res;
    res.H11 = bas(1) * bas(1) * b1.H11 + 2 * bas(2) * bas(2)
        - 2 * bas(1) * bas(2) * b1.L_inner;
    res.L_inner = bas(2);
    return res;
}
```

There is a similar routine `NewRight` for right blocks

We are now ready to define the main program: (file dmrqpb.cc)

First read in length, # of sweeps, and initialize array of blocks:

```
int main()
{
    Block siteblock;
    cerr << "Input length, number of iterations: ";
    int i, length, nsweeps;
    cin >> length >> nsweeps;
    cout << "length, nsweeps = " << length SP nsweeps << endl;
    cout << "Exact energy = " << exacten(length) << endl;
    exlen = length;
    Array1<Block> allblocks(length);
    WaveFunction psi;
    Real energy;
```

- `cout`, `cerr` statements are C++ “print”, `cin` reads in variables, `SP` is macro printing one space
- `Array1<Block>` defines 1D array of `Blocks`

Next, do “warmup” sweep, building from 4 sites to full size:

```
// Warmup sweep
  allblocks[1] = siteblock;
  for(i = 1; i < length/2; i++)
  {
    Block rightblock = allblocks(i).Reflect();

    System S(allblocks(i),siteblock,siteblock,rightblock);

    energy = S.GetGroundState(psi);
    cout << i+1 SP psi.v(2) SP energy SP 0 << endl;

    DensityMatrix rho(psi,Left);
    Vector basis = rho.NewBasis();

    allblocks[i+1] = NewLeft(allblocks(i),siteblock,basis);
  }
```

- Print step $\#$, g.s. energy, wave function at $\ell (= i + 1)$, iteration $\#$ ($= 0$ for warmup) at each step

Now do “finite system” iterations:

```
// Finite System sweeps
  for(int swp = 1; swp <= nsweeps; swp++)
  {
// We assume reflection symmetry:
    allblocks[length/2 + 2] = allblocks(length/2 - 1).Reflect();
    cout << endl;

// Right to left
    for(i = length/2+2; i > 3; i--)
    {
      System S(allblocks(i-3),siteblock,siteblock,allblocks(i));
      energy = S.GetGroundState(psi);
      cout << i-1 SP psi.v(3) SP energy SP swp - 0.5 << endl;

      DensityMatrix rho(psi,Right);
      Vector basis = rho.NewBasis();

      allblocks[i-1] = NewRight(siteblock,allblocks(i),basis);
    }
  }
```

- Start at symmetric configuration, use reflection symmetry

left to right half sweep analogous

```
// Left to right
cout << endl << 1 SP psi.v(1) SP energy SP swp << endl;
for(i = 1; i < length/2-1; i++)
{
    System S(allblocks(i),siteblock,siteblock,allblocks(i+3));
    energy = S.GetGroundState(psi);
    cout << i+1 SP psi.v(2) SP energy SP swp << endl;

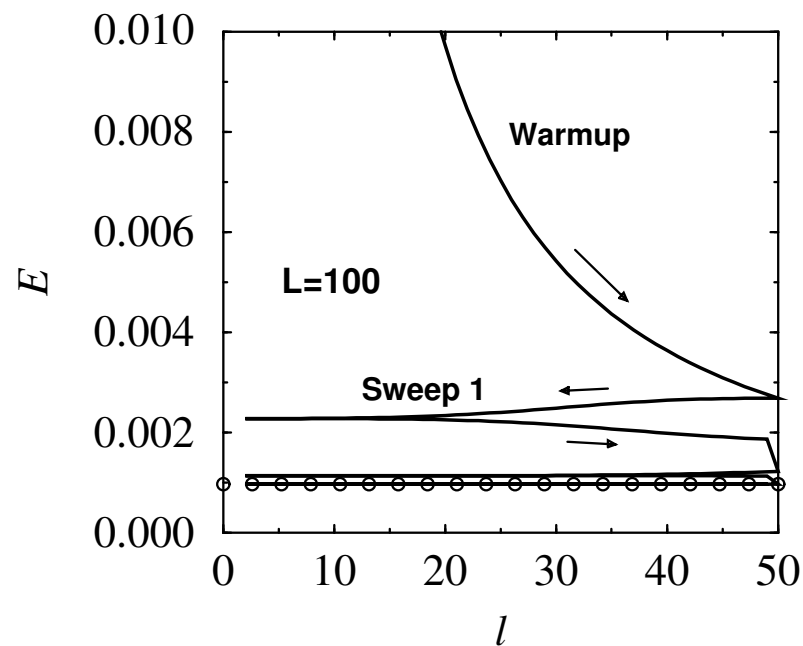
    DensityMatrix rho(psi,Left);
    Vector basis = rho.NewBasis();

    allblocks[i+1] = NewLeft(allblocks(i),siteblock,basis);
}
}
return 0;
}
```

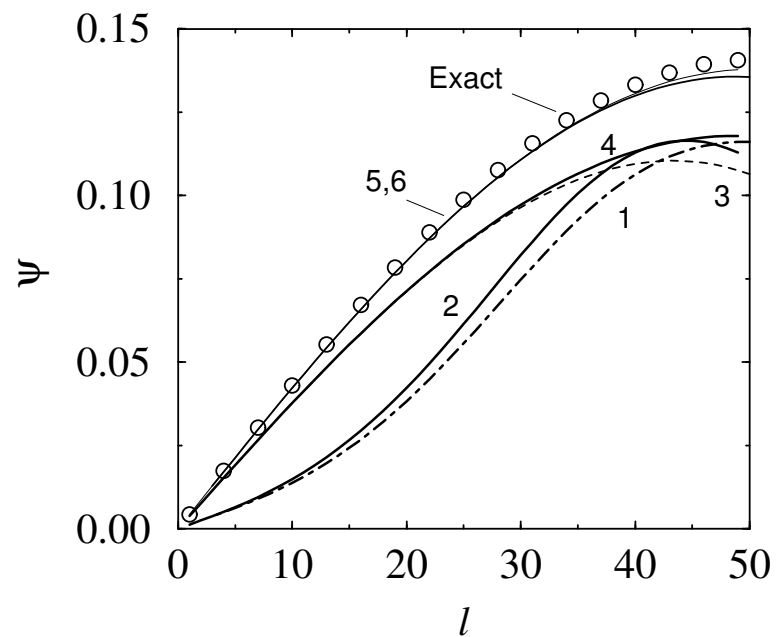
Behavior

$L = 100$, 6 finite-system sweeps

Ground-state energy:



Wavefunction:



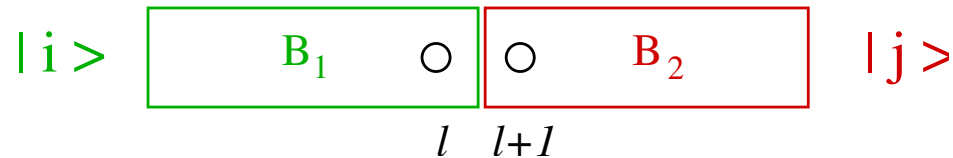
\Rightarrow near machine accuracy by diagonalizing only 4×4 matrix

IV (i) Programming Details

Concrete example: nearest-neighbor Heisenberg exchange

$$\mathbf{S}_\ell \cdot \mathbf{S}_{\ell+1} = S_\ell^z S_{\ell+1}^z + \frac{1}{2} (S_\ell^+ S_{\ell+1}^- + S_\ell^- S_{\ell+1}^+)$$

- Putting 2 blocks together



$$[H_{12}]_{ii';jj'} = [H_1]_{ii'} \delta_{jj'} + \delta_{ii'} [H_2]_{jj'} + [S_\ell^z]_{ii'} [S_{\ell+1}^z]_{jj'} + \frac{1}{2} \left([S_\ell^+]_{ii'} [S_{\ell+1}^-]_{jj'} + [S_\ell^-]_{ii'} [S_{\ell+1}^+]_{jj'} \right)$$

- Transforming operators:

Transformation matrix $O_{ij;\alpha}$ composed of m basis vectors u_{ij}^α with $\alpha = 1, \dots, m$ (usually density matrix eigenvectors)

Operator $A_{ij;i'j'}$ transformed via

$$A_{\alpha\alpha'} = \sum_{i,j,i',j'} O_{ij;\alpha} A_{ij;i'j'} O_{i'j';\alpha'}$$

Dimension of A : $(m_1 m_2) \times (m_1 m_2) \rightarrow m \times m$

Typically: B_1 left or right block, B_2 : added site

Efficiency

- Efficient multiplication of $H^{super}|\psi\rangle$ (needed for Lanczos ED)
- could construct (sparse) matrix for $H^{super} \Rightarrow$ inefficient
- instead generate terms from block operators

H for two block system can be written

$$[H]_{ij;i'j'} = \sum_{\nu} A_{ii'}^{\nu} B_{jj'}^{\nu}$$

(ν sum over all combinations of block operators in H)

$H\psi$ becomes

$$\sum_{i'j'} [H]_{ij;i'j'} \psi_{i'j'}^{\nu} = \sum_{\nu} \sum_{i'} A_{ii'}^{\nu} \sum_{j'} B_{jj'}^{\nu} \psi_{i'j'}.$$

Do j' sum then i' as sequence of 2 matrix–matrix products

\Rightarrow Reduces CPU as well as memory for most systems

- Computational cost: CPU $\sim Lm^3$ Memory $\sim m^2$

Efficiency (2)

- Using quantum numbers
 - Abelian quantum numbers like S^z and N_{ferm} good in any subsystem
 - \Rightarrow any basis can be partitioned by quantum number
 - \Rightarrow all operators consist of rectangular blocks that map between definite quantum numbers
 - Can store operators as collections of (dense) matrices, lists of quantum number pairs \Rightarrow C++ convenient
 - Above operations then have loops over quantum numbers
 - Nonabelian quantum numbers (e.g., \mathbf{S}^2) also possible, but more complicated
- Writing to disk

Information not used in current step can be written to disk
e.g., previously generated blocks in finite size algorithm

IV (ii) Measurements

- given state ψ_{ij} on two-block system

- single-site expectation value $\langle \psi | S_\ell^z | \psi \rangle$

$$\langle \psi | S_\ell^z | \psi \rangle = \sum_{i,i',j} \psi_{ij}^* [S_\ell^z]_{ii'} \psi_{i'j}$$

- correlation functions such as $\langle \psi | S_\ell^z S_m^z | \psi \rangle$

- ℓ and m on different blocks:

$$\langle \psi | S_\ell^z S_m^z | \psi \rangle = \sum_{i,i',j,j'} \psi_{ij}^* [S_\ell^z]_{ii'} [S_m^z]_{jj'} \psi_{i'j'}$$

- ℓ and m on the **same** block:

Incorrect for approximate ψ_{ij} :

$$\langle \psi | S_\ell^z S_m^z | \psi \rangle \approx \sum_{i,i',i'',j} \psi_{ij}^* [S_\ell^z]_{ii'} [S_m^z]_{i'i''} \psi_{i''j}$$

Reason: sum over i' should run over complete set of states, but it doesn't

Correct:

$$\langle \psi | S_\ell^z S_m^z | \psi \rangle = \sum_{i,i',j} \psi_{ij}^* [S_\ell^z S_m^z]_{ii'} \psi_{i'j}$$

General Rule: Compound operators internal to a block must be accumulated as the calculation proceeds

Almost all equal-time correlation functions can be generated like this

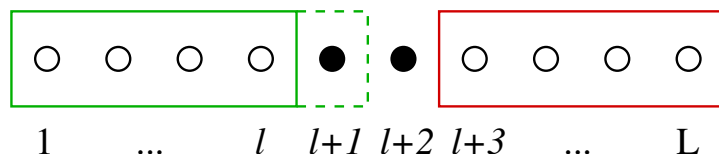
IV (iii) Wavefunction Transformations

$H^{super} \psi_T^k$ for Lanczos or Davidson costly (e.g., 40-100 steps)

Can be reduced if ψ_T^0 is a good guess for ψ_0

Good Guess: Use ψ_0 obtained from previous finite system step

\Rightarrow must transform ψ_0 obtained from step ℓ to $\ell + 1$ basis



Basis: $|\alpha_\ell s_\ell s_{\ell+1} s_{\ell+2} \beta_{\ell+3}\rangle = |\alpha_\ell\rangle \otimes |s_{\ell+1}\rangle \otimes |s_{\ell+2}\rangle \otimes |\beta_{\ell+3}\rangle$

Transform to: $|\alpha_{\ell+1} s_{\ell+2} s_{\ell+3} \beta_{\ell+4}\rangle$

Transformation of left basis:

$$|\alpha_{\ell+1}\rangle = \sum_{s_{\ell+1}, \alpha_\ell} L^{\ell+1} [s_{\ell+1}]_{\alpha_{\ell+1}, \alpha_\ell} |\alpha_\ell\rangle \otimes |s_{\ell+1}\rangle.$$

where $L^{\ell+1} [s_{\ell+1}]_{\alpha_{\ell+1}, \alpha_\ell} = u_{s_{\ell+1} \alpha_\ell}^{\alpha_{\ell+1}}$ (u_{ij}^α new basis vectors)

Similarly for right basis

$$|\beta_{\ell+3}\rangle = \sum_{s_{\ell+3}, \beta_{\ell+4}} R^{\ell+3} [s_{\ell+3}]_{\beta_{\ell+3}, \beta_{\ell+4}} |s_{\ell+3}\rangle \otimes |\beta_{\ell+4}\rangle$$

Superblock wavefunction:

$$|\psi\rangle = \sum_{\alpha_\ell s_{\ell+1} s_{\ell+2} \beta_{\ell+3}} \psi(\alpha_\ell s_{\ell+1} s_{\ell+2} \beta_{\ell+3}) |\alpha_\ell s_{\ell+1} s_{\ell+2} \beta_{\ell+3}\rangle$$

Since there is a truncation, must approximate

$$\sum_{\alpha_{l+1}} |\alpha_{l+1}\rangle \langle \alpha_{l+1}| \approx 1$$

New wavefunction:

$$\psi(\alpha_{l+1} s_{l+2} s_{l+3} \beta_{l+4}) \approx \sum_{\alpha_l s_{l+1} \beta_{l+3}} L^{\ell+1}[s_{l+1}]_{\alpha_{l+1}, \alpha_l} \psi(\alpha_l s_{l+1} s_{l+2} \beta_{l+3}) R^{\ell+3}[s_{l+3}]_{\beta_{l+3}, \beta_{l+4}}$$

Perform in two steps:

1. intermediate result:

$$\psi(\alpha_{l+1} s_{l+2} \beta_{l+3}) = \sum_{\alpha_l s_{l+1}} L^{\ell+1}[s_{l+1}]_{\alpha_{l+1}, \alpha_l} \psi(\alpha_l s_{l+1} s_{l+2} \beta_{l+3})$$

2. then form

$$\psi(\alpha_{l+1} s_{l+2} s_{l+3} \beta_{l+4}) = \sum_{\beta_{l+3}} \psi(\alpha_{l+1} s_{l+2} \beta_{l+3}) R^{\ell+3}[s_{l+3}]_{\beta_{l+3}, \beta_{l+4}}$$

- Analogous transformation is used in right to left steps
- Transformation relatively inexpensive in CPU and memory
- Since ψ_T^0 is physically close to ψ_0 , Davidson convergence criterium can be relaxed without converging to wrong state
- All transformations can be stored on disk
 - ⇒ arbitrary operators can be reconstructed *after* final ψ_0 is obtained, at end
 - ⇒ Number of $H\psi_T^k$ steps can be greatly reduced

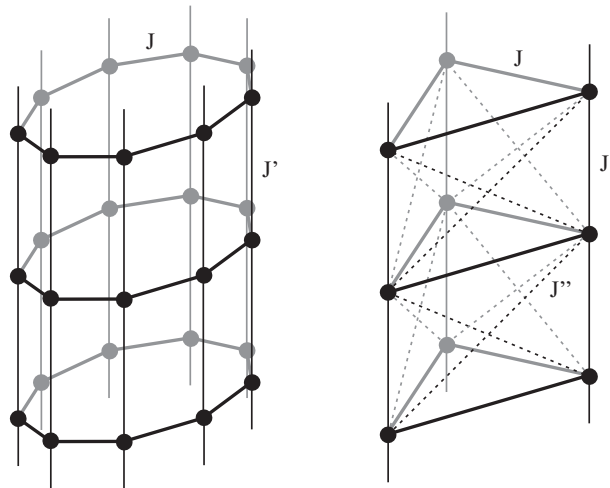
Application: Vanotubes

(Luscher, Noack, Misguich, Kotov, Mila, cond-mat/0405131)

$\text{Na}_2\text{V}_3\text{O}_7$

$\text{V}^{4+}: S = \frac{1}{2}$

spin tubes
with $J \gg J'$



effective 3-chain model

Ring with odd number of $S = \frac{1}{2}$ spins: 4-fold degenerate

$$H_{\text{eff}} = K \sum_{r=1}^{N-1} \mathbf{S}_r \cdot \mathbf{S}_{r+1} \left(1 + \alpha (\tau_r^+ \tau_{r+1}^- + \tau_r^- \tau_{r+1}^+) \right)$$

\mathbf{S}_r : spin, τ_r chirality on a ring: $S = \frac{1}{2}$ pseudospin

strong ring coupling: $\alpha \geq 4$ (3 legs, $J'' = 0$)

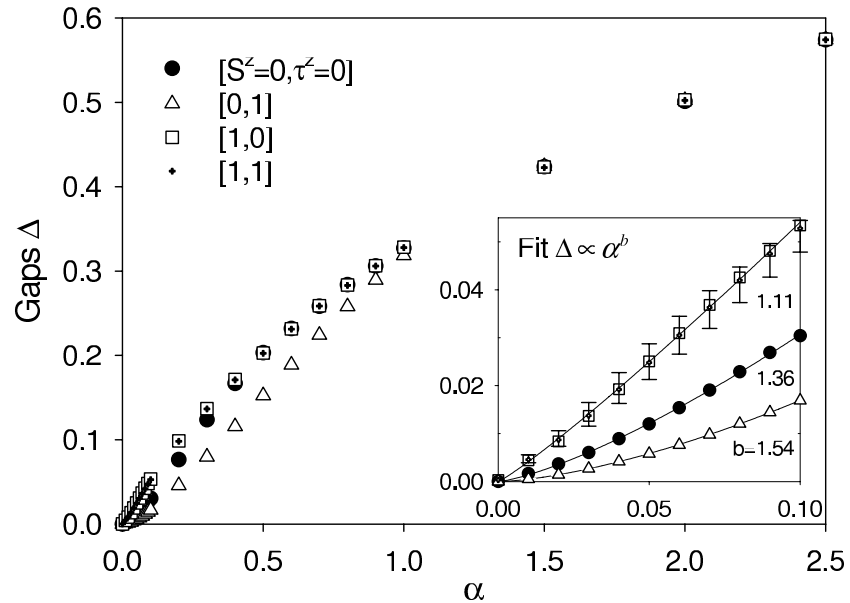
Bosonization (Schulz 1996), DMRG (Kawano & Takahashi, 1997): spin gap

Experiment (susceptibility, NMR): no spin gap (Gavilano *et al.*, 2003)

\Rightarrow effect of frustration? $\alpha \ll 4$

spin and chirality gaps
in $[S^z, \tau^z]$ sectors

- ⇒ chirality excitation $[0,1]$
lowest for $\alpha < 1$
- ⇒ gaps vanish as $\alpha \rightarrow 0$



$\alpha = 0.1$

character of the states:

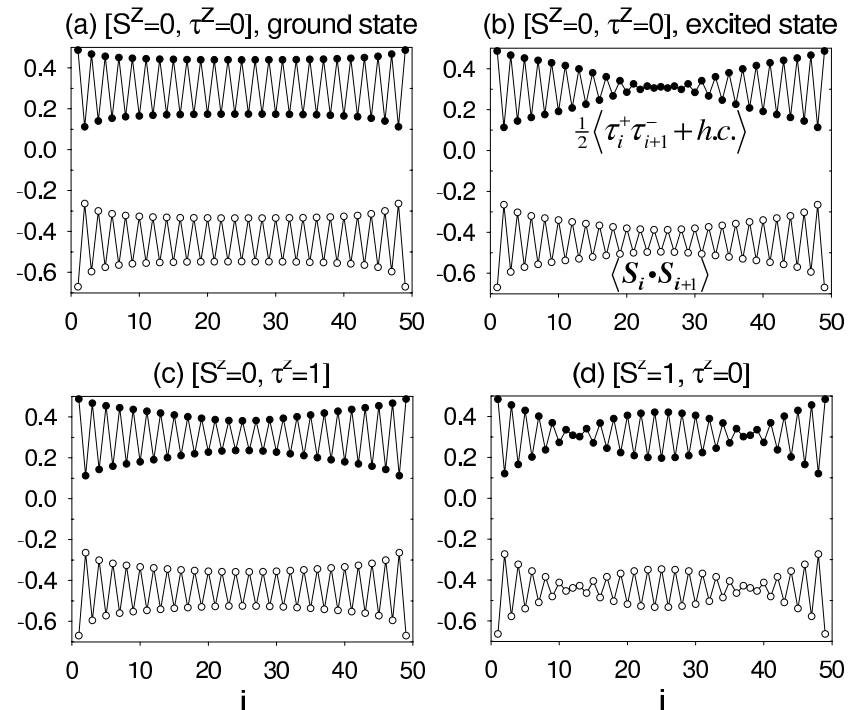
$$\langle \psi_n | \tau_i^+ \tau_{i+1}^- + \tau_i^- \tau_{i+1}^+ | \psi_n \rangle$$

$$\langle \psi_n | \mathbf{S}_i \cdot \mathbf{S}_{i+1} | \psi_n \rangle$$

$[0,0]$: dimerized

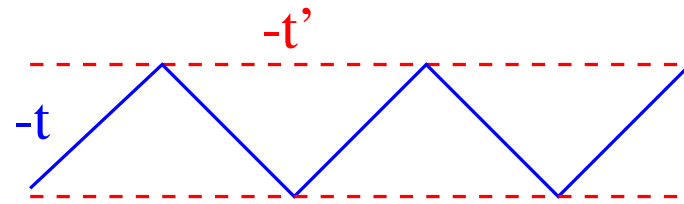
$[0,1]$: bound soliton pair

$[1,0]$: free solitons



Application: frustrated Hubbard chain

t - t' - U Hubbard chain:



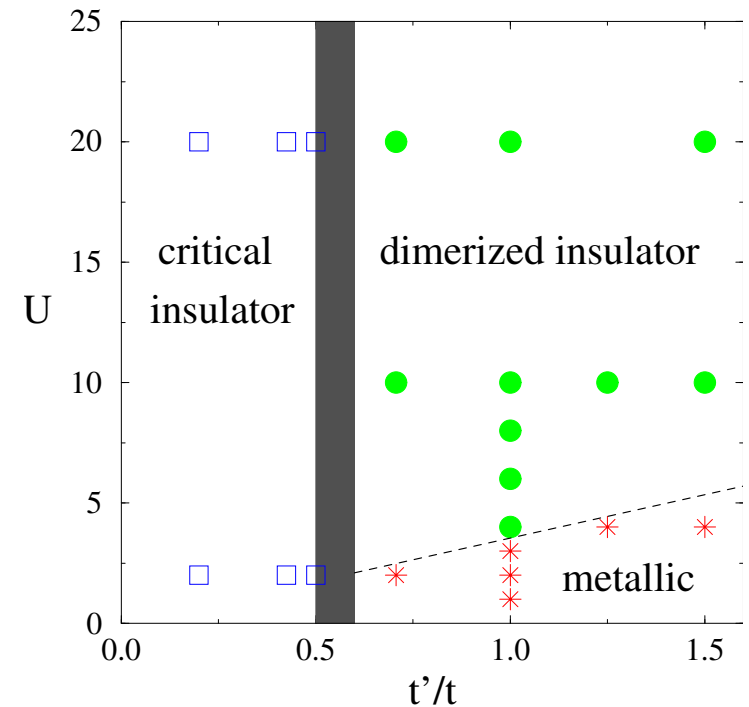
$$H = - \sum_{i,\sigma} (t c_{i\sigma}^\dagger c_{i+1\sigma} + t' c_{i\sigma}^\dagger c_{i+2\sigma} + \text{h.c.}) + U \sum_i n_{i\uparrow} n_{i\downarrow}$$

Dispersion: $\varepsilon(k) = -2t \cos k - 2t' \cos 2k \quad (t = 1)$

Ground-state phase diagram, $n = 1$:
(Daul and Noack, 1999)

Behavior as a function of U :

- $t' < 0.5$: 1D Hubbard, $U_c = 0$
 $\Delta_s = 0, \Delta_c > 0$
- $t' > 0.5$: Mott-Hubbard transition at $U_c > 0$
 $\Delta_s > 0, \Delta_c = 0 \rightarrow \Delta_c > 0$



Quantum Critical Behavior

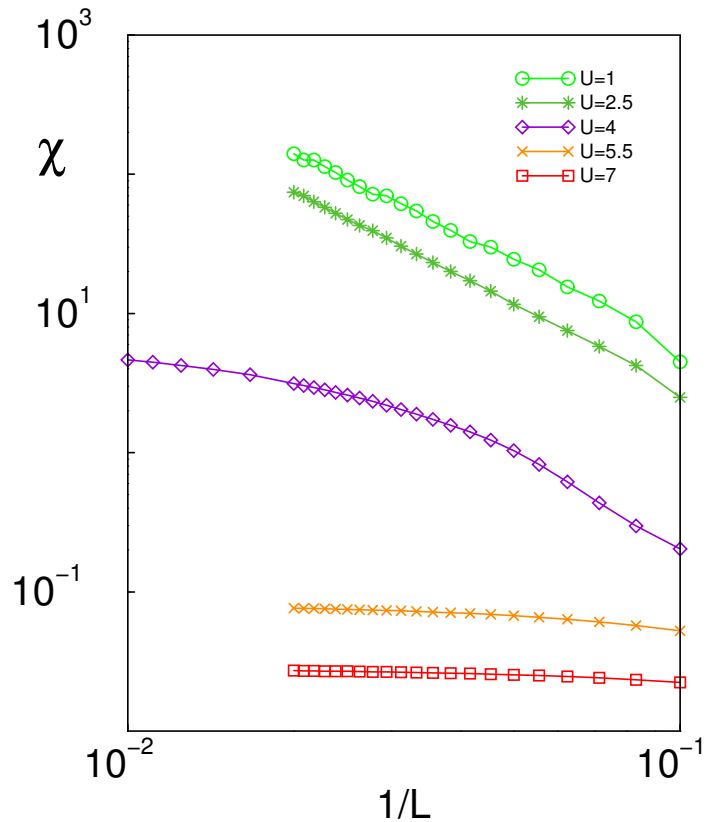
(Aebischer, Baeriswyl, & Noack, 2001)

Metal-Insulator transition as a function of U

Electric susceptibility:

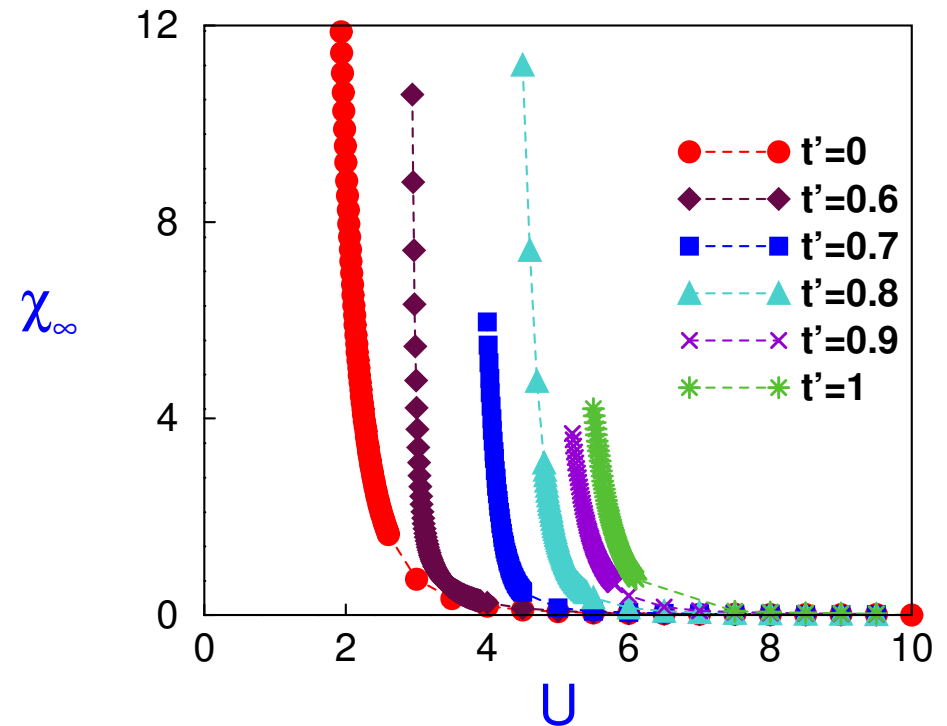
$$\chi = \left. \frac{\partial \langle \mathcal{P} \rangle}{\partial E} \right|_{E=0} = - \left. \frac{1}{L} \frac{\partial^2 E_0(E)}{\partial E^2} \right|_{E=0} \approx \frac{1}{LE} \sum_i x_i \langle n_i \rangle$$

Finite-size scaling:



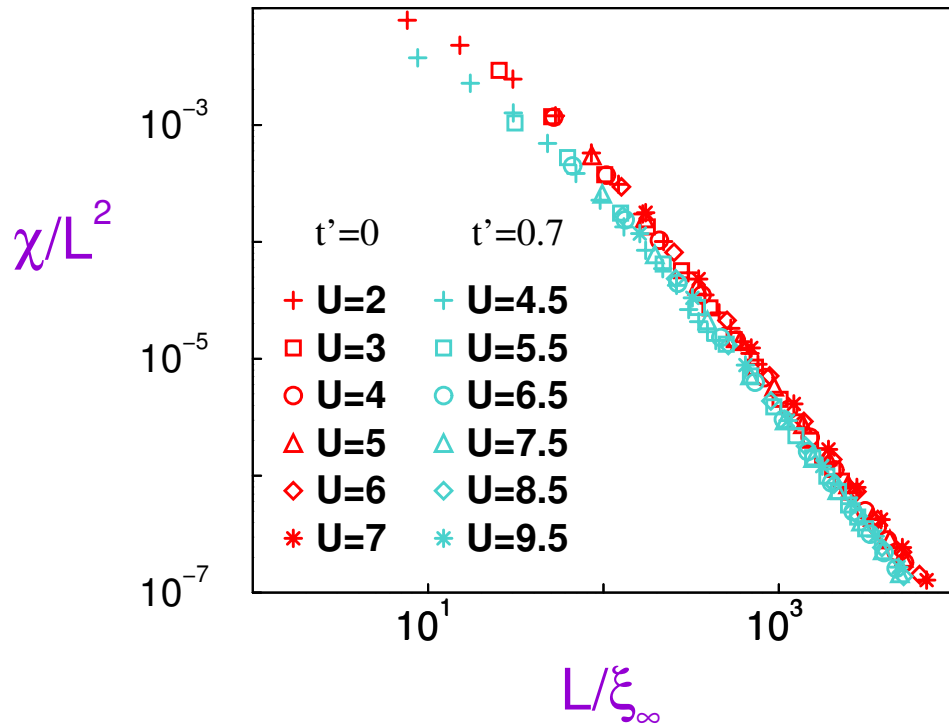
metal
 $\chi \sim L^2$
 critical
 insulator:
 $\chi \rightarrow \text{const.}$

Extrapolated value:



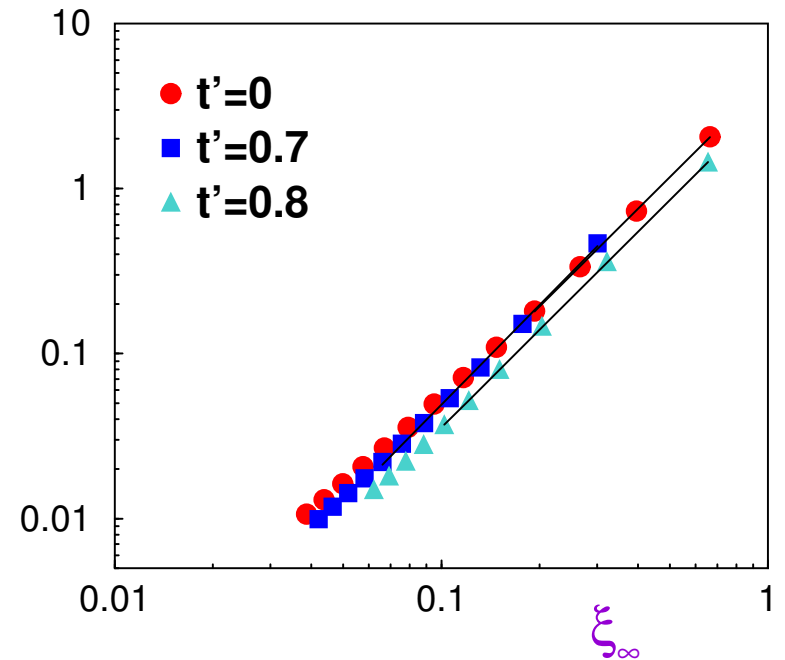
Form: $\chi_\infty \propto \exp\left(\frac{4\pi}{U - U_c}\right)$

Scaling Analysis



finite-size scaling: $\frac{\chi}{L^2} = C(t')\Phi(L/\xi_\infty)$

(Privman & M.E. Fisher, 1984)



$$\Rightarrow \chi_\infty \propto \xi_\infty^2$$

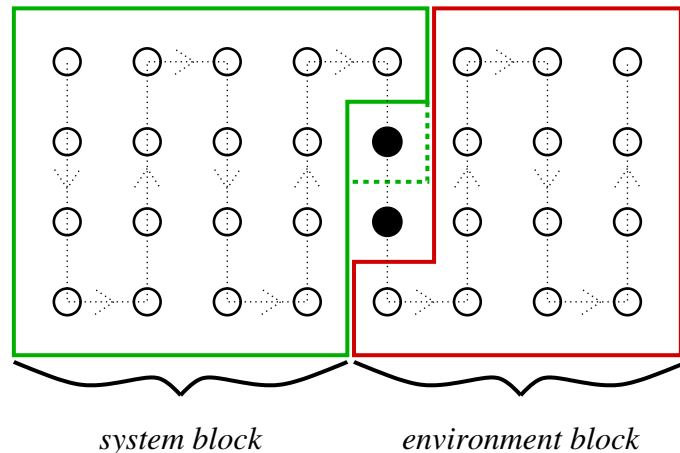
hyperscaling: $\chi_\infty \sim \xi_\infty^{2+z-d}$

(Kim & Weichman, 1991)

Further work: doping ($n < 1$) \Rightarrow itinerant ferromagnetism at large U/t !

IV (iv) Extensions – 2D and Fermion Systems

(Noack, White, Scalapino, 1994)



- 1D algorithm “folded” into 2D
- finite system algorithm necessary

- convergence depends strongly on width of system
⇒ exponential in width for spinless fermions (Liang & Pang 1994)

Applications:

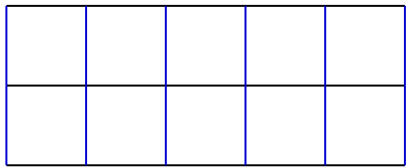
- Heisenberg, Hubbard and t - J -ladders; 2D t - J -model
 SrCu_2O_3 , $\text{Sr}_2\text{Cu}_3\text{O}_5$, $\text{Sr}_{14-x}\text{Ca}_x\text{Cu}_{24}\text{O}_{41-\delta}$
 NaV_2O_5 , CaV_2O_5 , high- T_c superconductors
- Kondo lattice model, periodic Anderson model
heavy fermion systems (CeAl_3 , UPt_3)
- Quantum Hall systems (Shibata & Yoshioka, 2001)

Spin Chains and Ladders

(White, Noack & Scalapino, 1994)

Heisenberg model on $n_c = 1, 2, 3, 4$ chains

$$H = J_{\parallel} \sum_{j=i+\hat{x}} \mathbf{S}_j \cdot \mathbf{S}_i + J_{\perp} \sum_{j=i+\hat{y}} \mathbf{S}_j \cdot \mathbf{S}_i$$

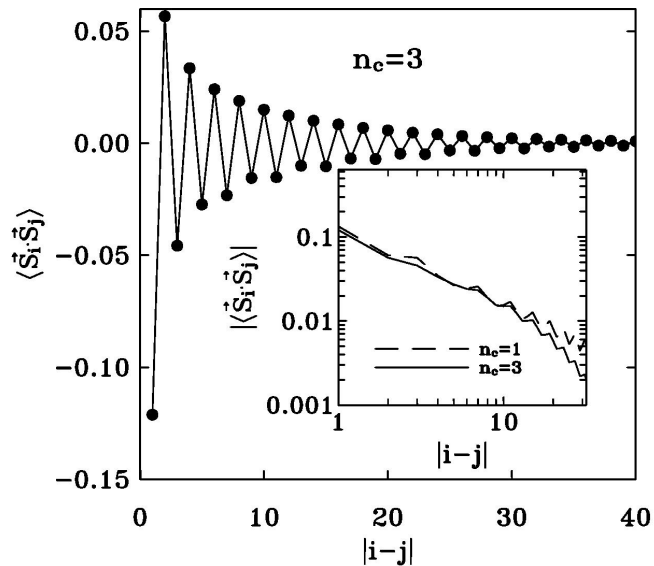


$n_c = 3$

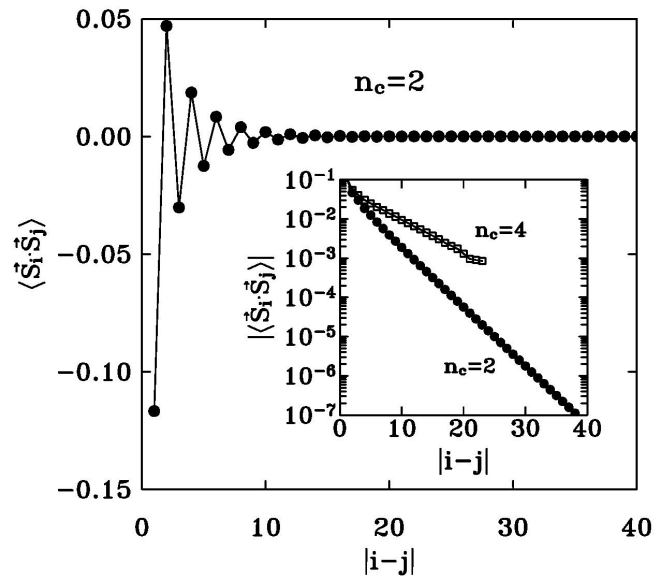


$n_c = 2$

Spin-spin correlation functions



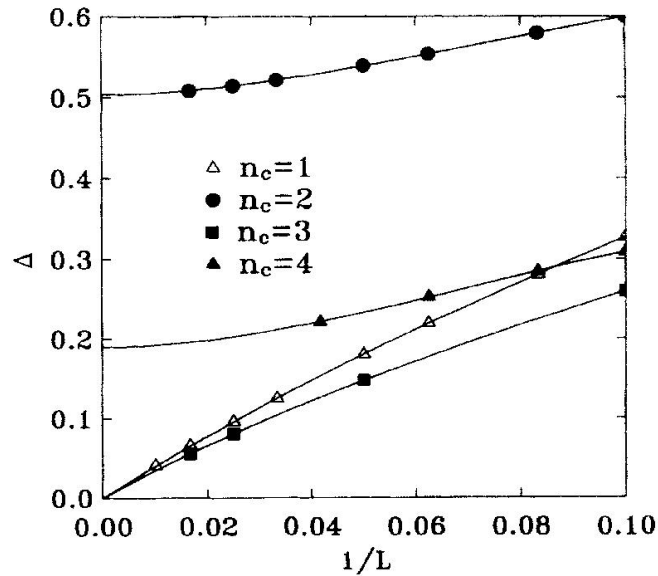
power law – critical



exponentially decaying – disordered

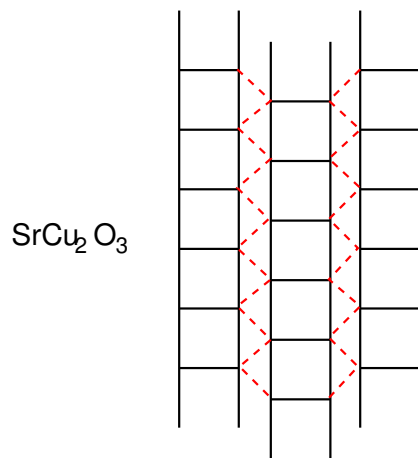
Spin excitations

$$\Delta = E_0(S = 1, L) - E_0(S = 0, L)$$

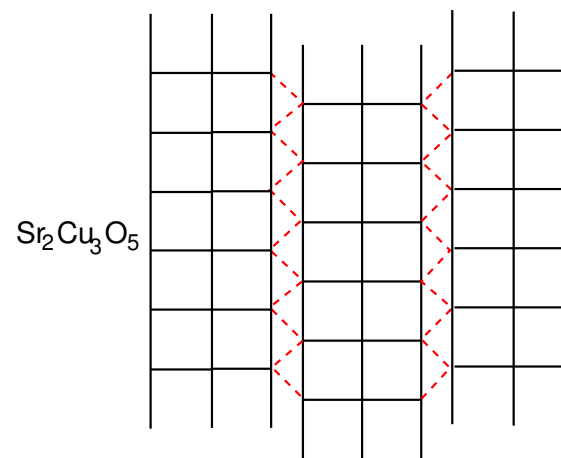


- $\Delta = 0, n_c$ odd
 - $\Delta > 0, n_c$ even
 - $J_{\perp} \gg J_{\parallel}$ limit:
 - $n_c = 2$: rung $S = 0$ singlet
 - $n_c = 3$: rung effective spin-1/2
- ⇒ Quantum effect – Haldane gap

Spin ladder materials



spin gap



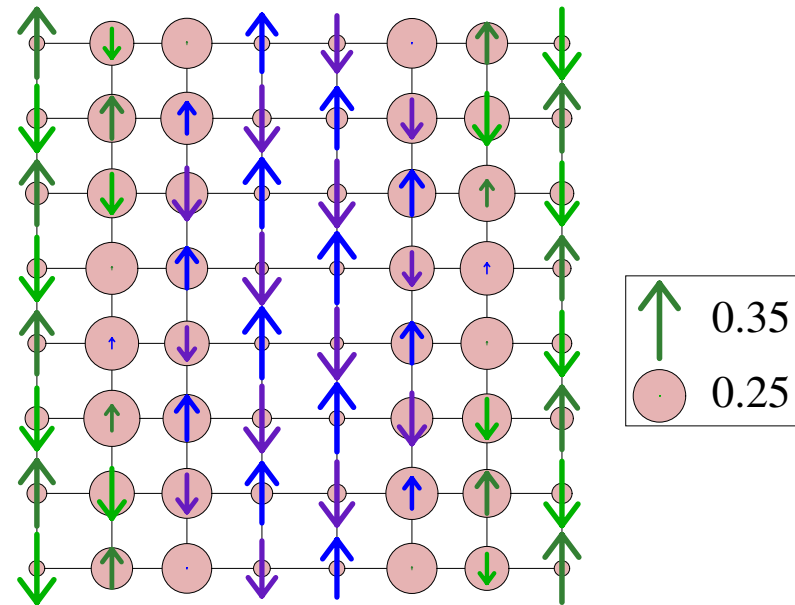
no spin gap

2D t - J Model

(White & Scalapino, 1998)

Stripe formation - high- T_c ?

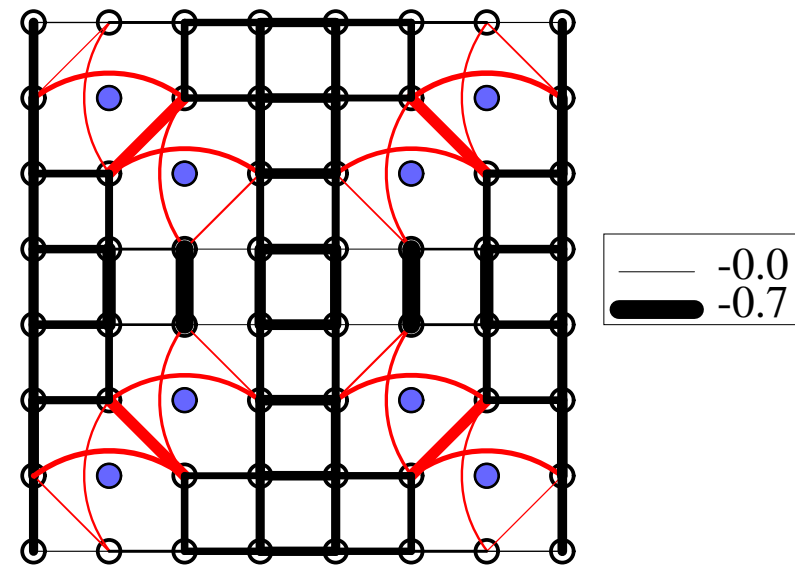
- 16×8 lattice (cylinder)
- doping $x = 1/8$
- circles: charge density
arrows: spin density
- domain walls: π -phase, $1/2$ -filled, bond centered
- site-centered, diagonal walls also possible



- 8×8 cylinder, 8 holes
- blue circles: most probable hole position
- lines: AF exchange strength

General conclusions:

- stripes w/o long-range Coulomb
- competition with $d_{x^2-y^2}$ pairing
- stripes “evaporate” with t'
(sign \rightarrow electron-doping)



Hubbard Model in Momentum Space

(Xiang, 1996; Nishino, Jeckelmann, Gebhard & Noack, 2002)

$$H = \sum_{k\sigma} \varepsilon_k c_{k\sigma}^\dagger c_{k\sigma} + \frac{U}{N} \sum_{pkq} c_{p-q\uparrow}^\dagger c_{k+q\downarrow}^\dagger c_{k\downarrow} c_{p\uparrow}$$

Method: choose a 1D path in k -space, similar to 2D algorithm in real space

- advantages
 - convergence only weakly dependent on dimensionality (enters only in ε_k)
 - method exact in weak coupling
 - momentum is a conserved quantity
- disadvantages: interaction non-local
 - convergence poor at large U/t
 - bookkeeping for the interaction terms

⇒ more accurate than real-space DMRG for sufficiently small U

2D square lattice, periodic BCs: $U/t \approx 8$

- current research: more general models

$$\sum_{pkq} V_{\sigma\sigma'}(q) c_{p-q\sigma}^\dagger c_{k+q\sigma'}^\dagger c_{k\sigma} c_{p\sigma}$$

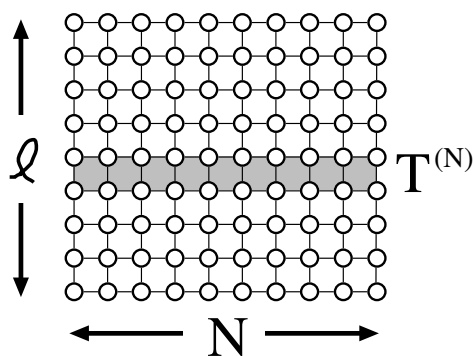
V (i) Classical Transfer Matrices

1D Quantum Systems closely related to 2D classical systems

Row Transfer Matrix

(Nishino, 1995)

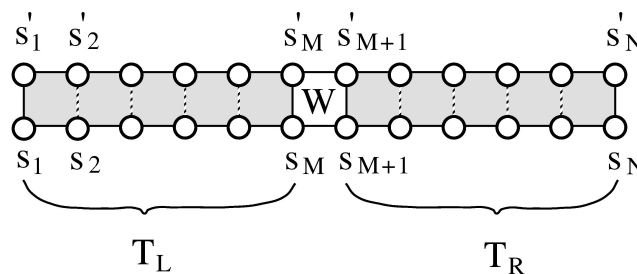
Ising model on a cylinder (periodic in ℓ)



Row transfer matrix $T^{(N)}(\mathbf{s}'|\mathbf{s})$
has dimension 2^N

\Rightarrow Treat $T^{(N)}$ using DMRG

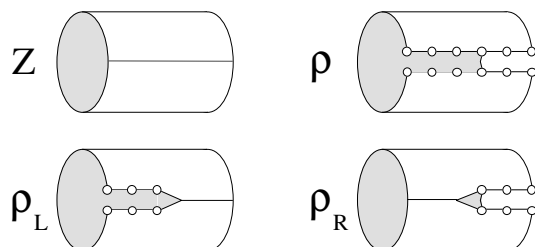
Can divide into two parts:



$$T^{(N)}(\mathbf{s}'|\mathbf{s}) = T_L(\mathbf{s}'_L|\mathbf{s}_L)W(s'_M s'_{M+1}|s_M s_{M+1})T_R(\mathbf{s}'_R|\mathbf{s}_R)$$

Partition function:

$$Z = \text{Tr} \rho = \text{Tr}(T^{(N)})^\ell = \sum_{\alpha} \lambda_{\alpha}^{\ell}$$



For $\ell \gg N$, only largest eigenvalue λ_1^{ℓ} is important \Rightarrow Use DMRG to obtain λ_1^{ℓ}

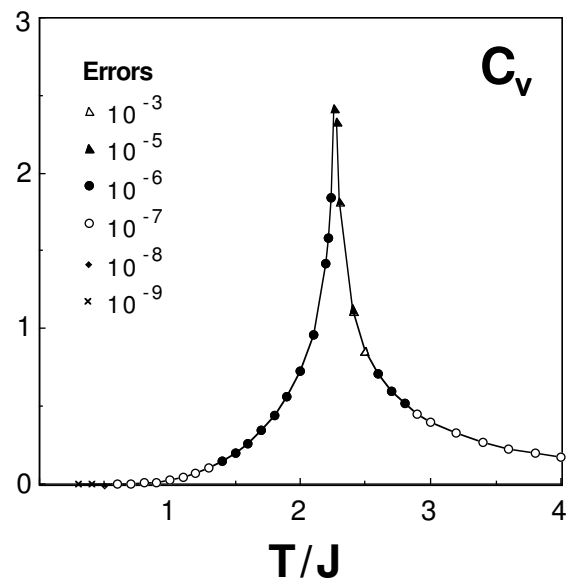
Can define reduced transfer matrices ρ_L, ρ_R

Both infinite and finite system algorithms can be used

Example:

(Nishino, 1995)

Specific heat for the 2D Ising model

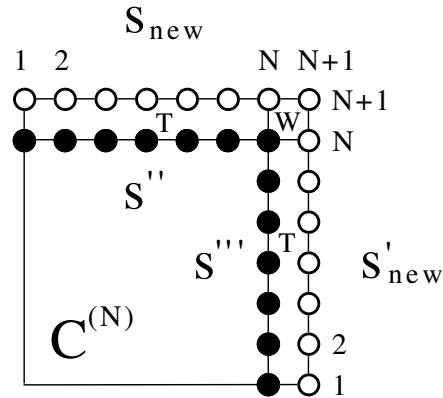


Corner Transfer Matrix:

(Nishino and Okunishi, 1996)

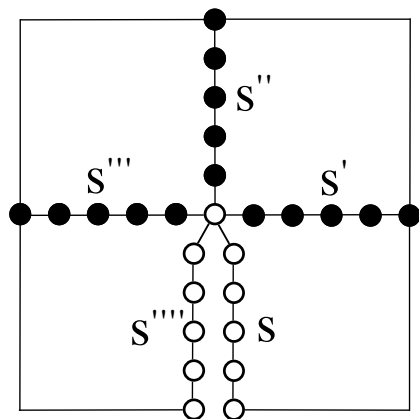
Can also treat Corner Transfer Matrix

(Baxter, 1968)



Variational partition function fourth power of C.T.M.

$$Z^{(2N-1)} = \text{Tr} \rho_c \approx \text{Tr} \left(\tilde{C}_c^{(N)} \right)^4 = \sum_{\nu=1}^m \alpha_{\nu}^4$$



Baxter treated $N \rightarrow \infty$ limit variationally

\Rightarrow Equivalent to infinite system algorithm (Okunishi, 1996)

However, $\tilde{C}_c^{(N)}$ need not be explicitly diagonalized!

V (ii) Finite Temperature

Simplest idea: Use Boltzmann weight $e^{-\beta E_\alpha}$ to weight target states $|\psi^\alpha\rangle$ in mixed density matrix:

$$\rho_{ii'} = \sum_{\alpha} e^{-\beta E_{\alpha}} \sum_j \psi_{ij}^{\alpha} \psi_{i'j}^{\alpha*}$$

Refinement: (Moukouri and Caron, 1996)

Target $M \sim 10 - 30$ states with weight $1/M$, project to smaller Hilbert space by forming

$$\boxed{\bar{H}_B} \quad \boxed{\bar{H}_B}$$

\Rightarrow *Fully* diagonalize H_{BB} , calculate Boltzmann sum

$$\langle A \rangle = \sum_{\gamma} e^{-\beta E_{\gamma}} \langle \psi_{BB}^{\gamma} | A | \psi_{BB}^{\gamma} \rangle$$

Idea: Basis of \bar{H}_B good description of *all* states

Advantages

- Straightforward extension of original DMRG
- Most accurate at low T (on finite system)

Disadvantages

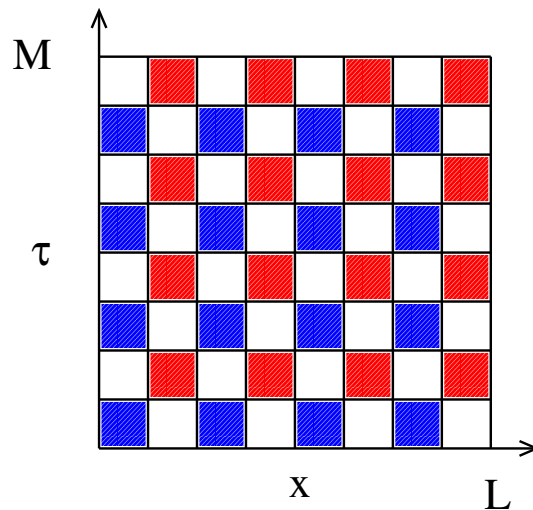
- Finite-size effects (largest at small T)
- Not clear whether high- T limit converges

Transfer Matrix DMRG (TMRG)

(Bursill *et al.*, 1996)
(Wang and Xiang, 1997)

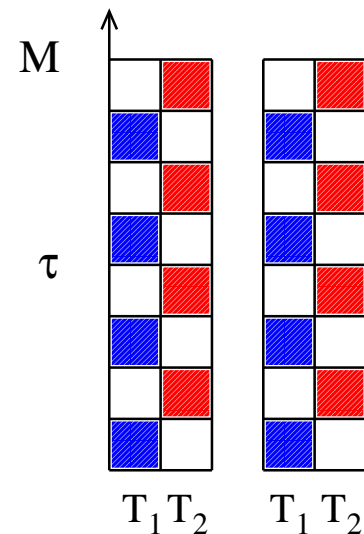
Idea: Treat quantum system as 1 + 1 dimensional classical system using Trotter–Suzuki (checkerboard) decomposition

$$Z = \text{Tr} e^{-\beta H} = \text{Tr}(e^{-\Delta\tau H_{\text{odd}}} e^{-\Delta\tau H_{\text{even}}})^{M/2} + \mathcal{O}(\Delta\tau^2)$$



Transfer Matrix in *space* direction:

$$Z_M^\infty = \lim_{L \rightarrow \infty} \text{Tr} (T_1 T_2)^{L/2}$$



Obtain partition function for *infinite* system at finite T

Free energy related to largest eigenvalue of transfer matrix

$$F = - \lim_{\Delta\tau \rightarrow 0} \frac{\ln \lambda_{\max}}{2\beta}$$

⇒ Use DMRG to obtain λ_{\max}

Advantages

- In thermodynamic limit – calculates properties of infinite system
- Exact at high T
- Can calculate thermodynamic properties easily
- τ -dependence available for local dynamics
 - Must analytically continue $i\omega_m \rightarrow \omega + i\delta$
(Maximum Entropy)
 - Spatial (or k) dependence more difficult

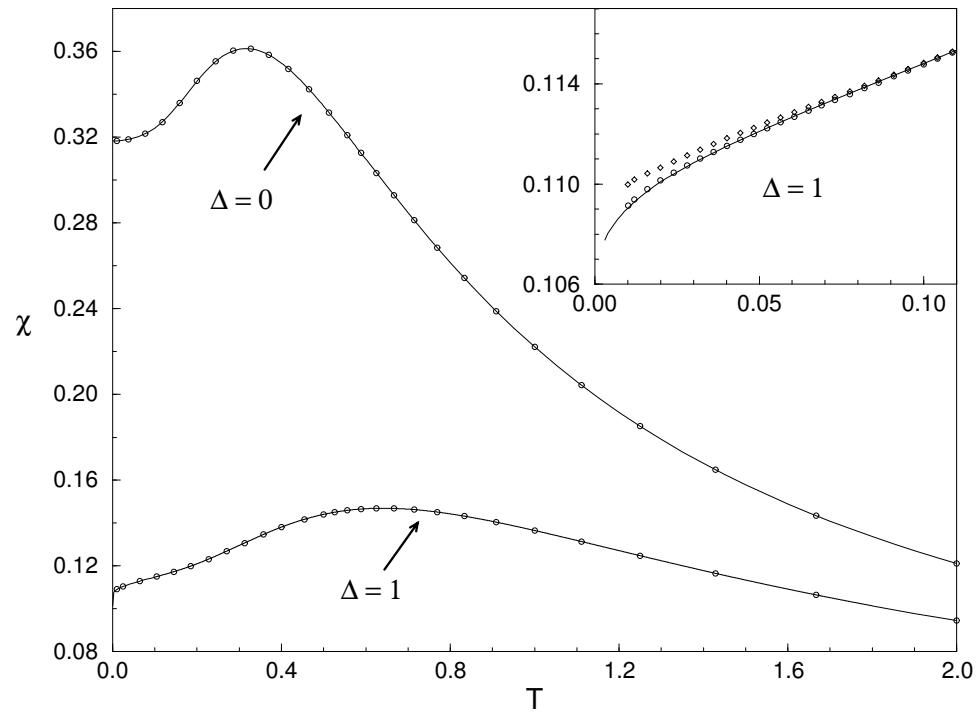
Disadvantages

- Technical difficulties – $(T_1 T_2)$, ρ not symmetric in general
- Must extrapolate to $\Delta\tau \rightarrow 0$
- Lower temperature more difficult – “size” $\iff T$
- Longer distance correlation functions more difficult

Example

(Wang and Xiang, 1997)

Wang et al Fig. 3



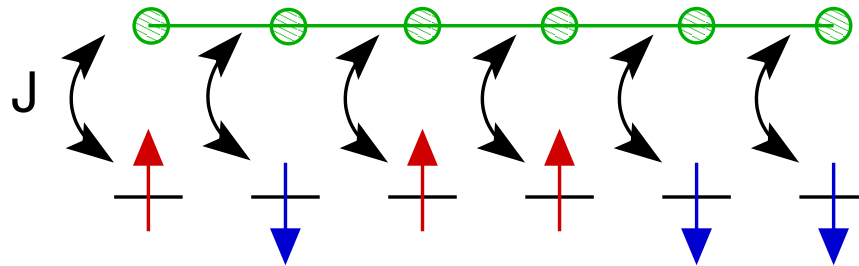
Spin Susceptibility for the spin-1/2 XY ($\Delta = 0$) and Heisenberg chains

1D Kondo Lattice Model

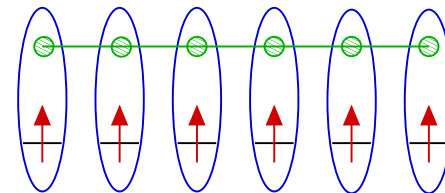
(Shibata & Tsunetsugu, 1999)

Hamiltonian

$$H = -t \sum_{i,\sigma} \left(c_{i,\sigma}^\dagger c_{i+1,\sigma} + \text{h.c.} \right) + \frac{J}{2} \sum_i \mathbf{S}_i \cdot \left(c_{i,\alpha}^\dagger \boldsymbol{\sigma}_{\alpha,\beta} c_{i,\beta} \right)$$

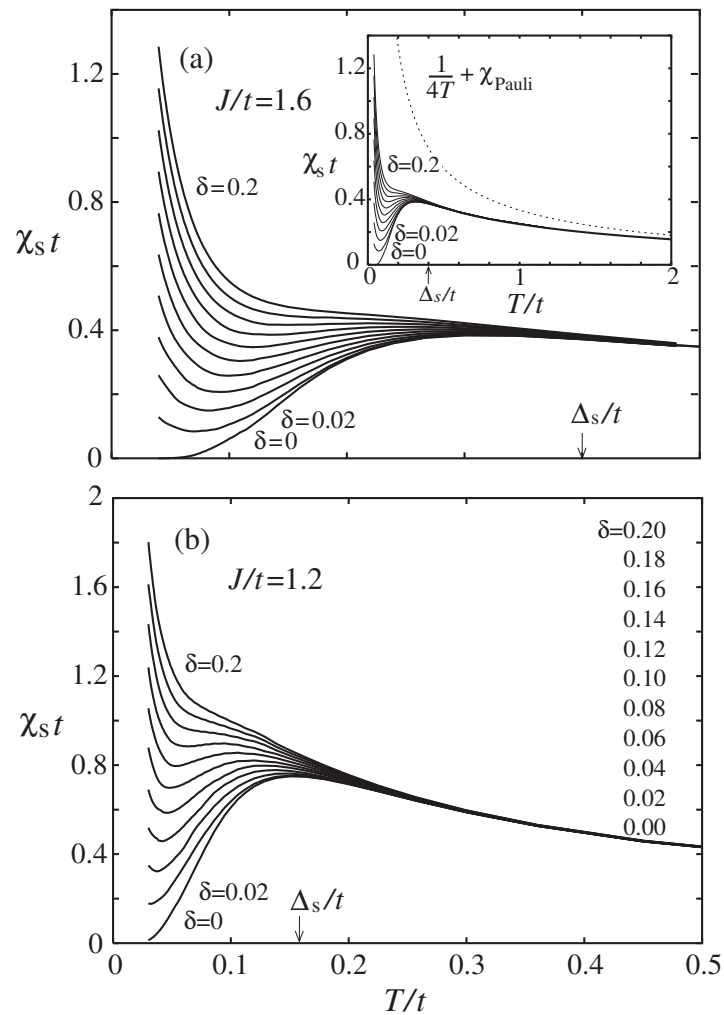


- Single 1D conduction band
- Localized spin-1/2 impurity at each site
- Half-filling ($\langle n \rangle = 1$): Kondo insulator: localized singlets $\Delta_c > \Delta_s > 0$



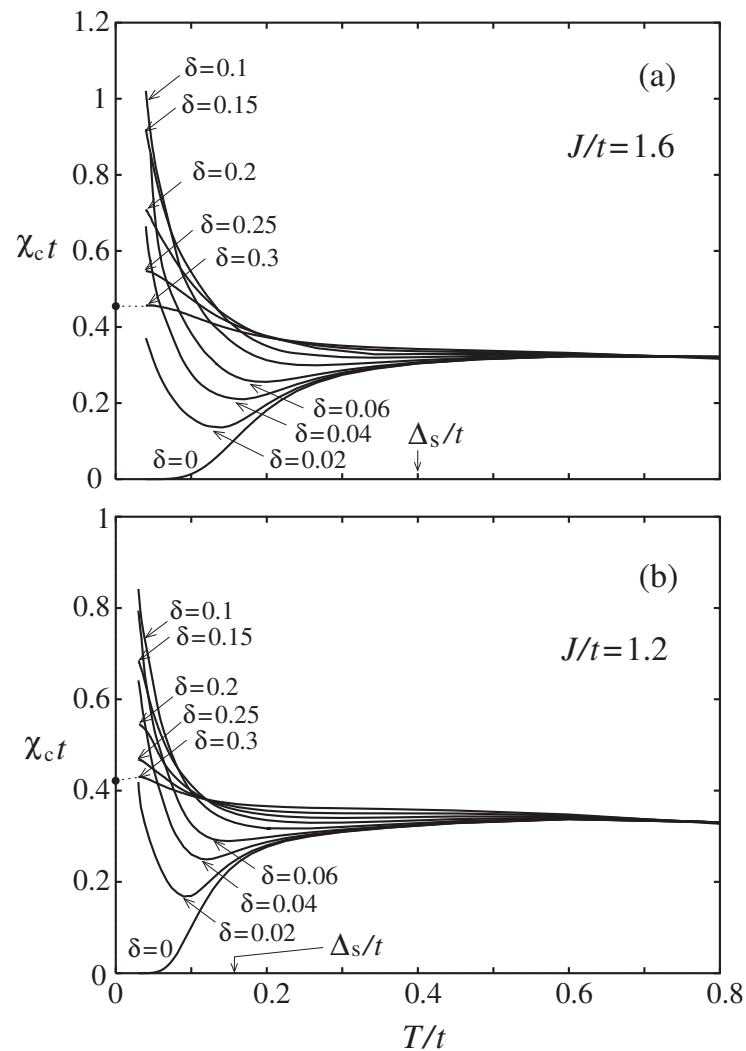
- doping ($\langle n \rangle = 1 - \delta$): crossover to metallic behavior (RKKY Luttinger liquid)

Spin susceptibility



- high T : $\chi_s = \chi_{\text{Pauli}} + \chi_{\text{Curie}}$
- low T , $\delta = 0$: spin gap
- low T , $\delta > 0$: crossover to metal

Charge susceptibility



- high T : free electron behavior
- low T , $\delta = 0$: charge gap
- low T , $\delta > 0$: crossover to metal

V (iii) Dynamics of a Quantum System

dynamical correlation function

$$G(\mathbf{k}, \omega) = \langle \psi_0 | A_{\mathbf{k}}^\dagger (\omega + i\eta - H)^{-1} A_{\mathbf{k}} | \psi_0 \rangle$$

additional density-matrix eigenstates must be “targetted”:

- Lanczos vector method (Hallberg, 1995)

target vectors: Krylov basis

$$|\psi_0\rangle, A_{\mathbf{k}}|\psi_0\rangle, H A_{\mathbf{k}}|\psi_0\rangle, H^2 A_{\mathbf{k}}|\psi_0\rangle, \dots$$

- correction vector method: (White & Kühner, 1999)

target vectors:

$$|\psi_0\rangle, A_{\mathbf{k}}|\psi_0\rangle, (\omega + i\eta - H)^{-1} A_{\mathbf{k}}|\psi_0\rangle$$

⇒ more accurate, but more costly: different run for each ω

- minimization method (Jeckelmann, 2002)

correction vector minimizes functional

$$W_{A,\eta}(\omega, \psi) = \langle \psi | (E_0 + \omega - H)^2 + \eta^2 | \psi \rangle + \eta \langle A | \psi \rangle + \eta \langle \psi | A \rangle$$

to get spectral weight

$$W_{A_{\mathbf{k}},\eta}(\omega, \psi_{\min}) = -\pi\eta \operatorname{Im} G(\mathbf{k}, \omega)$$

⇒ minimization more stable and efficient than matrix inversion

Example: Single-Particle Spectral Weight for Hubbard Chain

(Benthien, Gebhard, & Jeckelmann, 2004)

1D Hubbard model (open BCs)

$$H = -t \sum_{\ell=1, \sigma}^{L-1} \left(c_{\ell, \sigma}^{\dagger} c_{\ell+1, \sigma} + c_{\ell+1, \sigma}^{\dagger} c_{\ell, \sigma} \right) + U \sum_{\ell=1}^L n_{\ell, \uparrow} n_{\ell, \downarrow}$$

Single-particle spectral weight for holes (photoemission)

$$A(k, \omega) = \frac{1}{\pi} \text{Im} \langle \psi_0 | c_{k, \sigma}^{\dagger} \frac{1}{H + \omega - E_0 + i\eta} c_{k, \sigma} | \psi_0 \rangle$$

where $c_{k, \sigma} = \frac{1}{\sqrt{L}} \sum_{\ell} e^{ik\ell} c_{\ell, \sigma}$ (assumes periodic BCs)

Problem: open BCs

Solution: use particle-in-a-box states

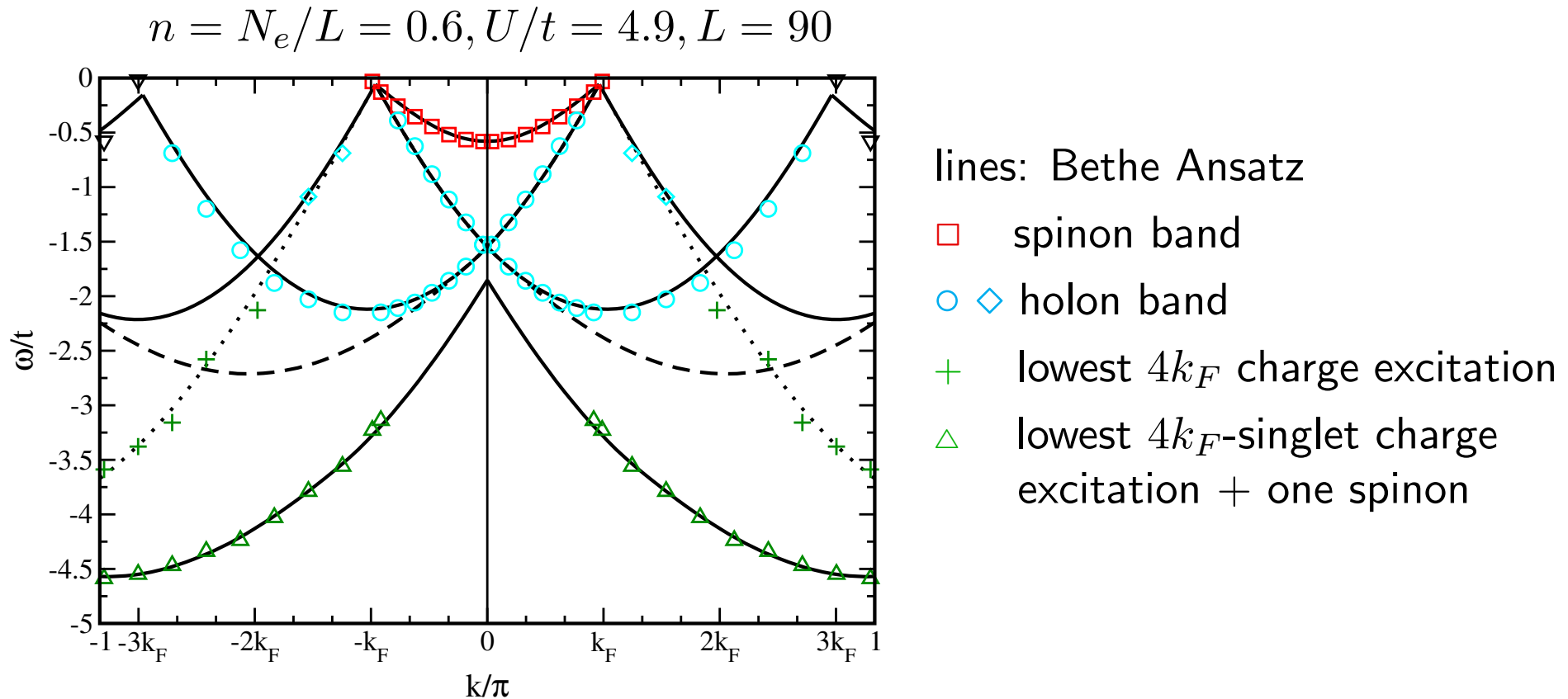
$$c_{k, \sigma} = \sqrt{\frac{2}{L+1}} \sum_{\ell} \sin(k\ell) c_{\ell, \sigma}$$

⇒ What does $A(k, \omega)$ look like in a Luttinger liquid?

(Spin-charge separation, no fermionic quasiparticle, ...)

Comparison with Bethe Ansatz

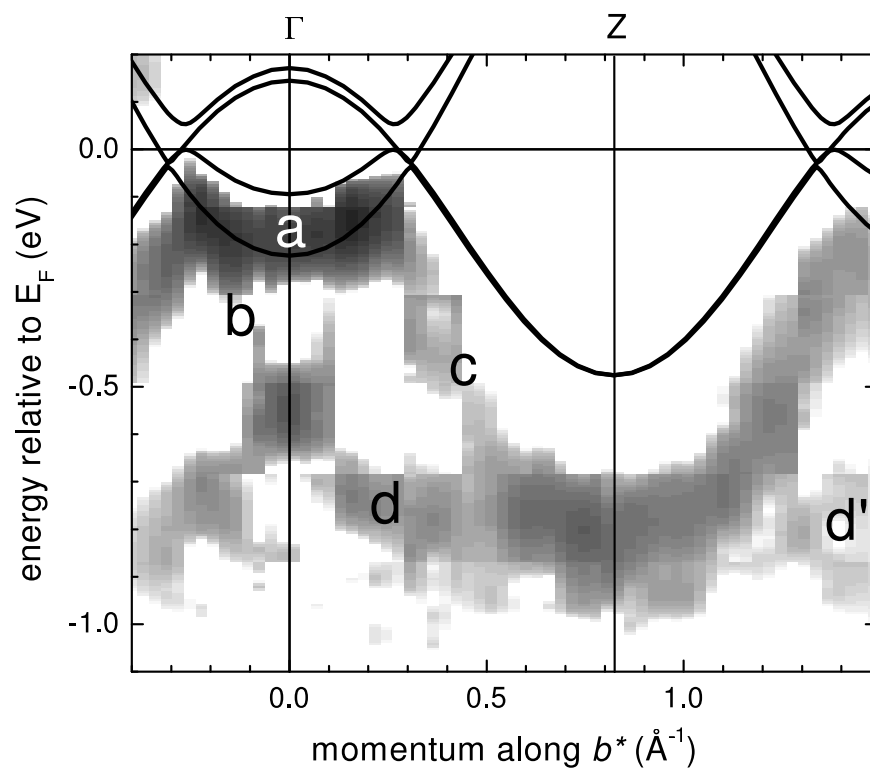
Bethe Ansatz: dispersion of specific excitations (no spectral weight)



⇒ excellent agreement with Bethe Ansatz dispersion

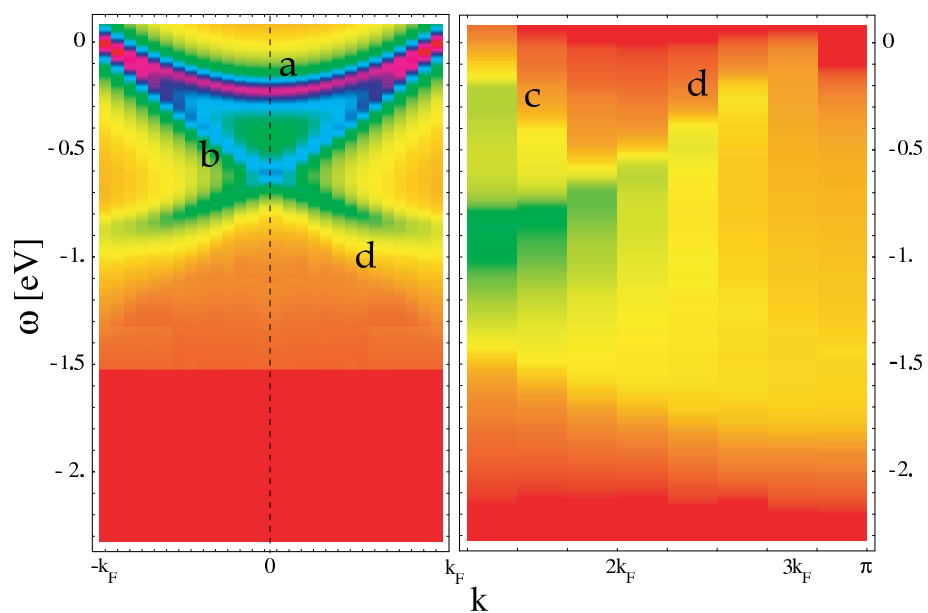
Comparison with ARPES on TTF-TCNQ

ARPES



(Sing *et al.*, 2003)

DDMRG



V (iv) Quantum Chemistry

(White & Martin, 1999)

$$H = \sum_{i,j,\sigma} t_{ij} c_{i\sigma}^\dagger c_{j\sigma} + \frac{1}{2} \sum_{i,j,k,l} G_{ijkl} \sum_{\sigma,\sigma'} c_{i\sigma}^\dagger c_{j\sigma'}^\dagger c_{k\sigma'} c_{l\sigma}.$$

- $c_{i\sigma}^\dagger$ creates electron in molecular orbital i (N orbitals)
- t_{ij} single-electron integral of molecular orbitals i and j
- G_{ijkl} two-electron integral (Coulomb repulsion)
 - ⇒ exact diagonalization: “full CI”
- Method: similar to momentum-space, 2D methods
- Computational cost: $(N^4 m^2 + N^3 m^3)$
- Applications
 - H_2O (White & Martin, 1998)
 - CH_4 , HHeH (Daul, Ciofini, Daul, & White, 2000)
 - Be_2 , N_2 , HF (Mitrushenkov et al., 2001)
 - CH_2 , F_2 , LiF (Legeza, Röder, & Hess, 2002; 2003)
 - ionic-neutral crossing in LiF : potential to 10^{-6} , dipole moment to 10^{-5}
 - Ne , H_2O , N_2 , C_2H_4 , H_2 -chains (Chan & Head-Gordon, 2002)
- ⇒ energies compare well to full CI (up to 6 digits of accuracy)

Site Ordering Problem

Which orbitals should be placed near one another?

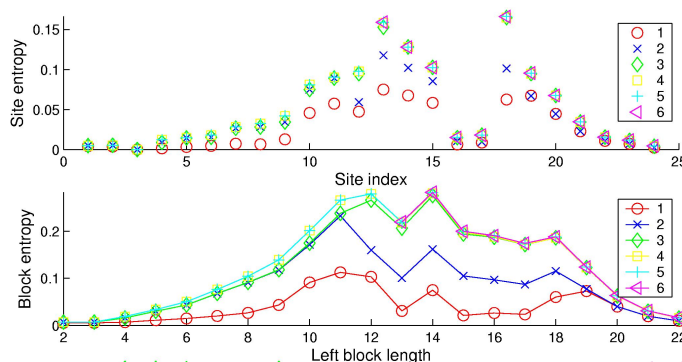
- single-site Density Matrix ρ_p (Legeza & Solyom, ...)



$\Rightarrow S(\rho_p)$: influence of site p

site entropy $S(\rho_p)$

block entropy $S(\rho_A)$



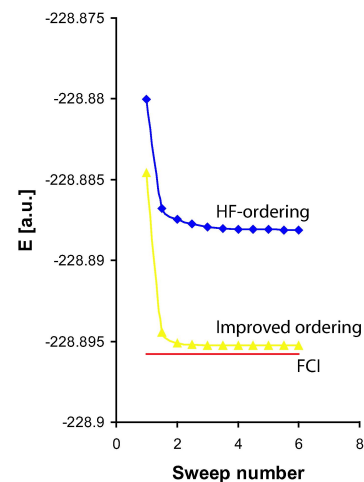
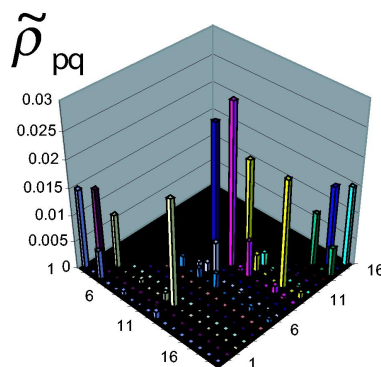
H₂O molecule

- two-site density matrix $\rho_{p,q}$ (Rissler, White & RMN, ...)



\Rightarrow effective interaction between p and q

Fluorine
18 orbitals
 $m = 200$



V (v) Time Evolution

Time evolution of a state in quantum mechanics

$$|\psi(t)\rangle = e^{-iHt} |\psi(0)\rangle$$

typically: $H = H_0 + H_1 \Theta(t)$, $|\psi(0)\rangle = |\psi_0\rangle$ or $A^\dagger |\psi_0\rangle$

DMRG approaches:

- Runge-Kutta integration of $|\psi_0\rangle_{\text{DMRG}}$ (Cazallila & Marston, 2002)
 \Rightarrow only good for small times t
- division of e^{-iHt} into 2-site terms
(White & Feiguin, 2004; Daley, *et al.*, 2004)
Trotter-Suzuki decomposition, 2-site parts exactly applied \Rightarrow quantum gates
- expansion of e^{-iHt} in Krylov basis (Schmitteckert, cond-mat/0403759)
(Manmana, Muramatsu & Noack, ...)
multi-target method – optimal targetting under development

Applications: tunnel current between Luttinger liquids,
transport current in a quantum dot
Bose-Hubbard model: Bose-Einstein condensation, atom traps

V (vi) Matrix Product States

DMRG changes the state of the system block in 2 steps:

1. blocking (add a site to a block)

$$|\alpha\rangle_l \otimes |s_l\rangle \rightarrow |\beta'_{l+1}\rangle$$

2. truncation (in density matrix eigenbasis)

$$|\beta_{l+1}\rangle = u_{\beta'}^{\beta} |\beta'_{l+1}\rangle$$

Both steps can be combined (as in wavefunction transformations)

$$|\beta_{l+1}\rangle = \sum_{s_l, \alpha} A_{\beta\alpha}^s |\alpha\rangle_l \otimes |s_l\rangle$$

$A_{\beta\alpha}^s$ is a matrix which maps from α_l to β_{l+1}

The DMRG wavefunction can be written as a sum of such products

(Ostlund & Rommer, 1995)

$$|\psi_{\text{MPS}}\rangle = \sum_{\{s_l\}} \text{Tr} \{ A^{s_1} A^{s_2} A^{s_3} \dots A^{s_L} \} |s_1, s_2, \dots, s_L\rangle$$

The A^{s_l} are $m \times m$ matrices, except for A_1 & A_L which are m -element *vectors*

This is a special case of a *matrix product state*

The DMRG is a variational calculation in the space of such states

Features

- Any state can be described as a MPS (with dimension of A^{s_ℓ} large enough)
- Some states are very compactly described:
 - Néel state $|\uparrow\downarrow\uparrow\downarrow\uparrow\dots\rangle$
 - Bell state $|\uparrow\uparrow\uparrow\dots\rangle \pm |\downarrow\downarrow\downarrow\dots\rangle$
 - AKLT state: product of singlets to describe spin-1 chain
 $\Rightarrow 2 \times 2$ matrices
- Matrix product states can be variationally optimized using different methods
 - power method $H^n |\psi_{\text{MPS}}\rangle$
 - imaginary time evolution $e^{-\Theta H} |\psi_{\text{MPS}}\rangle$
 - Lanczos
 - DMRG – very efficient, but complicated
- an arbitrary operator X can be evaluated directly in terms of matrix products
 \Rightarrow Calculations with matrix product states generalize DMRG

Are other MPS's better than the DMRG state for particular problems?

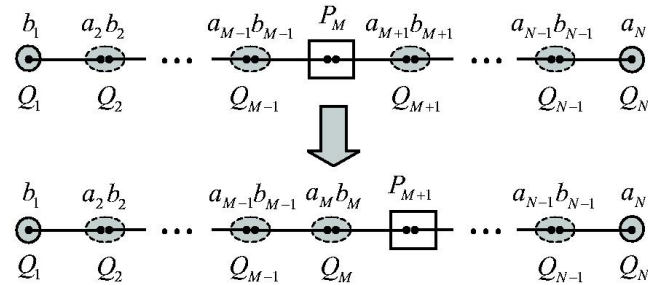
Answer: yes (almost certainly)

Better Matrix Product-like States

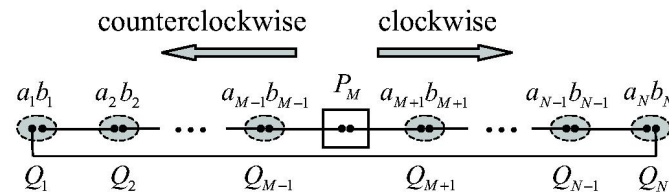
Periodic boundary conditions

(Verstraete, Porras & Cirac, c-m/0404706)

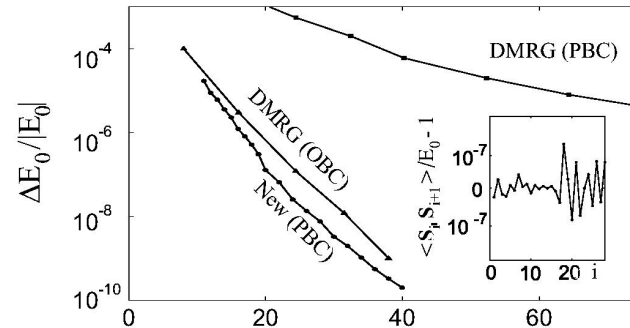
DMRG



New Method



Results: $L = 28$ Heisenberg chain

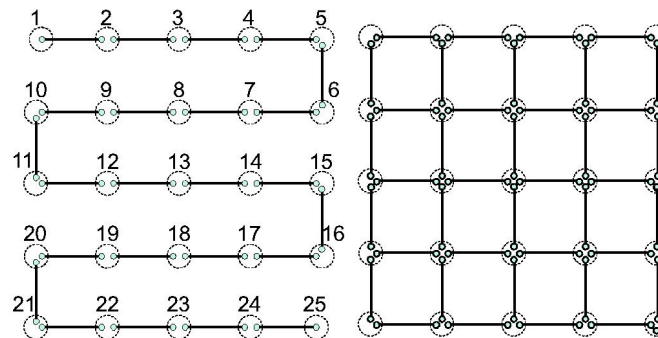


Questions:

- computational cost - matrices no longer sparse
- optimal minimization algorithms?

Application to other systems

- Finite temperature or dissipation
(Verstraete, García-Ripoll & Cirac, cond-mat/0406426)
- 2D systems
(Verstraete, & Cirac, cond-mat/0407066)



Entanglement in all 4 directions \Rightarrow Tensor product states needed!

DMRG and Quantum Information

Application of Quantum Information in the DMRG

- entanglement (von Neumann) entropy $S_A = -\text{Tr} \rho_A \ln \rho_A = S_B$

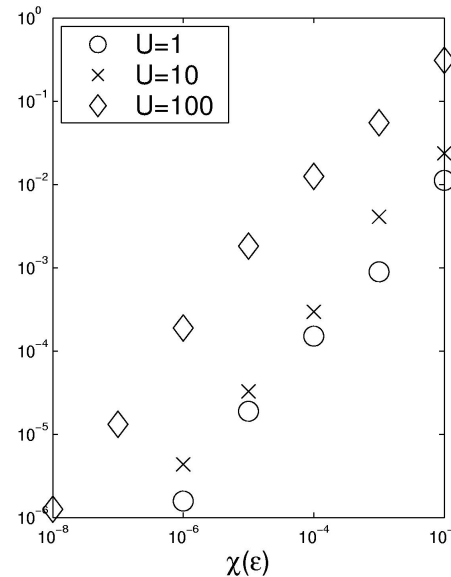
Error in E_0

vs.

Change in ρ_A after truncation

1D Hubbard model, $L = 80$

(Legeza & Solyom, 2004)



\Rightarrow How does ρ_A depend on characteristics of system?

Applications of the DMRG in Quantum Information Theory

- decoherence
 - \Rightarrow DMRG simulation of entanglement with environment
- foundations of quantum information theory
 - example: bounds on information content of a noisy channel

Discussion: DMRG

- DMRG is now a “standard method” for 1D+ spin and fermion systems
- Basic algorithm can still be improved, for example through better use of symmetries (S^2 , lattice symmetries, ...)
- Biggest challenge: more efficient extension to 2D+ or 3D+ (classical systems) lattices
- Currently under development:
 - more general models in momentum space
 - quantum chemistry: more realistic systems
 - dynamics of quantum systems: efficiency can be improved, many possibilities for applications
 - transfer matrices: improved dynamics, more systems
 - non-equilibrium systems: new field!
- Exciting new ideas (from Quantum Information Theory)
 - Matrix and tensor product states \Rightarrow generalizations of DMRG
 - Prospects for
 - periodic boundary conditions
 - 2D systems
 - finite temperature, dissipative systems